四、高空圖分析原理與應用

四、1地轉風與高度場分析

四、高空圖之分析和其原理　　C-1

(一)：高空等壓面上天氣圖的分析

* 要了解大氣之熱力性質，必須分析：氣壓場、氣溫、濕度、密度和位溫場。

* 若大氣適合流体靜力平衡，則氣壓和高度場為一對一之單調遞減函數，故可以用氣壓為垂直座標。∴在等壓面上，高度值較大的地方，就相當於等高面上的高壓位置；而高度值低的就相當於低壓位置(在等高面上)。

* 所以在等壓面上，由於理想氣体方程式 $(p=\rho RT)$ 知：

1) 密度只是氣溫的函數；即等密度線必平行等溫線；故不必再做密度場分析。
2) 又由位溫的定義 $\left[\theta = T\left(\frac{P_{00}}{P}\right)^{R/c_p}\right]$，在等壓面上等位溫線必平行等溫線，故也不需再做位溫場之分析。因此，若高空天氣圖採用等壓面圖，則只要分析高度、氣溫和濕度場即可。在作業上可方便許多。

* 另外，在中高緯度地區，大尺度大氣運動適合準地轉近似，故高度場即為準地轉運動之流場。

$$\because \nabla^2\psi = \zeta = \frac{1}{f}\nabla^2\Phi \ , \ \text{or} \ \psi' = \frac{\Phi'}{f} \quad : \text{geostrophy} \qquad —— ①$$

C-1：地轉風和高度場之分析

若大氣適合地轉風近似，在等壓面上地轉風之大小可由下式表示，

$$V_g = \frac{g}{f}\frac{\partial z}{\partial n} \simeq \frac{g}{f}\frac{\delta z}{\delta n} \qquad —— ②$$

∴若已知地轉風的大小，且相鄰兩條等高線的距離為 δn，而這兩條等高線之高度差為 δz (一般取 60 gpm)，則

$$\delta n = \frac{g}{f}\frac{\delta z}{V_g} \qquad —— ③$$

對上式做圖，可得不同緯度 (f) 之相鄰兩條等高線的距離和其間地轉風場大小的關係圖來。得同樣之 δn，在越高緯風速越小，∴在高空天氣圖分析時，要多利用地轉風大小來修正兩條等高線間之距離。

圖 C-1 可參考實習之天氣圖。

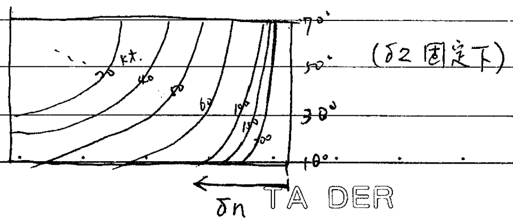

TA DER

（大動 §6.4.3 ageostropic wind）

* 当然，實際風和地轉風間会有差異，此差異向量稱為地轉偏差風（ageostrophic wind, $\vec{V}_{ag}$），即 $\vec{V}_{ag} = \vec{V} - \vec{V}_g$ —— ④

造成 $\vec{V}_{ag}$ 的因素有：(1) 地形，(2) 摩擦力的作用，及 (3) 發展迅速的天氣系統。

又由地轉風之定义：$f\hat{k}\times\vec{V}_g = -\nabla_p\Phi$ —— ⑤

∴ 運動方程式：$\frac{d\vec{V}}{dt} = -f\hat{k}\times\vec{V} - \nabla_p\Phi + \vec{F}_r = -f\hat{k}(\vec{V}-\vec{V}_g) + \vec{F}_r$

$= -f\hat{k}\times\vec{V}_{ag} + \vec{F}_r$ —— ⑥

故若大氣无摩擦力的作用（$\vec{F}_r = 0$），則單位質量大氣的加速度即為地轉偏差風的科氏力作用。

*（注意：大氣之加速度是由於科氏力、压力梯度力和摩擦力三力之不平衡所造成。）

* 若實際風和地轉風同向，但較強（$\vec{V} > \vec{V}_g$），則稱為超地轉風（super-geostrophic wind）。此時地轉偏差分量和實際風同向，但因科氏力之作用，使得大氣運動向右加速（見式6）。同理，$\vec{V} < \vec{V}_g$ 之次地轉風（subgeostrophic wind）則使大氣運動向左加速。

* 地轉偏差風之分量（即造成地轉偏差風之因素）：

由定义：$\vec{V} = \vec{V}_g + \vec{V}_{ag}$

$$\therefore \frac{d\vec{V}}{dt} = \frac{d\vec{V}_g}{dt} + \frac{d\vec{V}_{ag}}{dt} = -f\hat{k}\times\vec{V}_{ag} + \vec{F}$$

$$= \underbrace{\frac{\partial\vec{V}_g}{\partial t} + \vec{V}\cdot\nabla\vec{V}_g + \omega\frac{\partial\vec{V}_g}{\partial p}} + \underbrace{\frac{d\vec{V}_{ag}}{dt}} \quad —— ⑦$$

$$故 -f\hat{k}\times\vec{V}_{ag} = \underset{①}{\frac{\partial\vec{V}_g}{\partial t}} + \underset{②}{\vec{V}\cdot\nabla\vec{V}_g} + \underset{③}{\omega\frac{\partial\vec{V}_g}{\partial p}} + \underset{④}{\frac{d\vec{V}_{ag}}{dt}} - \underset{⑤}{\vec{F}_r} \quad —— ⑧$$

∴ 地轉偏差風可分為五個分量：

① 等變压風分量（isollobaric wind）　（$\frac{\partial p}{\partial t} = b$）or $\frac{\partial z}{\partial t}$

② 平流地轉偏差風分量（advective ageostrophic wind）

③ 对流 〃 〃 〃 〃 〃 〃（convective 〃 〃）

④ 地轉偏差变量分量，及 （$\vec{X}$）

⑤ 摩擦地轉偏差風分量（antitriptic wind）

即 $\vec{V}_{ag} = \vec{V}_{ag(i)} + \vec{V}_{ag(a)} + \vec{V}_{ag(c)} + \vec{V}_{ag(F)} + \vec{X}$ —— ⑨

TA DER

當摩擦力為0時，空氣運動的加速度即為壓力梯度力與科氏力的不平衡（地轉偏差風的科氏力作用）所造成。

(一) 摩擦地轉偏差風分量 (Antitriptic Wind)

摩擦力為減速力，它使空氣運動的速度減小，科氏力也 (压力场没有变化) 隨之減小，但壓力梯度力不受影響，如圖，科氏力、梯度力(压力) 與摩擦力平衡，因

$$-f\hat{k}\times\vec{V}_{ag(F)} = -\vec{F} \quad (\text{在无加速度时 } \frac{d\vec{V}}{dt}=0) \tag{6-26}$$

故摩擦力與摩擦地轉偏差風分量之科氏力，大小相等方向相反。因此，真實風總是比地轉風小，在北半球它偏向地轉風的左側。(即指向低压)

且 總

陸地上約為 40%
海上 約 60%

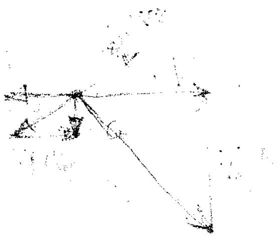

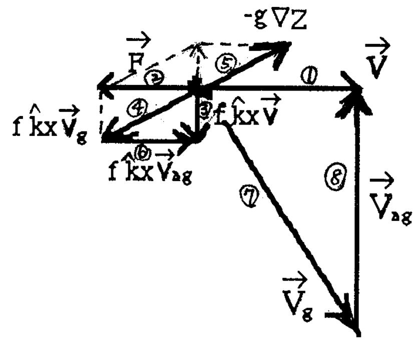

圖 6-5

(二) 等變壓風分量 (Isollobaric Wind)

$\nabla(\frac{\partial Z}{\partial t})$ app. $\quad \vec{V}_{ag(i)} = \frac{1}{f}\hat{k}\times\frac{\partial \vec{V}_g}{\partial t}$

當等變壓線 $\nabla(\frac{\partial Z}{\partial t})$ 的梯度很大時，等變壓風分量可能是地轉偏差風的主要部分。因 (地轉風隨時間之變化 ⇒ 如系統之發展等)

$$-f\hat{k}\times\vec{V}_{ag(i)} = \frac{\partial \vec{V}_g}{\partial t} \Rightarrow \vec{V}_{ag(i)} = \frac{1}{f}\hat{k}\times\frac{\partial \vec{V}_g}{\partial t} \tag{6-27}$$

由地轉平衡方程式

$$(-f\hat{k}\times\vec{V}_g = g\nabla Z) \quad \because \vec{V}_g = +\frac{g}{f}\hat{k}\times\nabla Z \quad \begin{cases} u_g = -\frac{1}{f}\frac{\partial\Phi}{\partial y} \\ v_g = \frac{1}{f}\frac{\partial\Phi}{\partial x} \end{cases} \tag{6-28}$$

故

$$\Rightarrow \vec{V}_{ag(i)} = \frac{1}{f}\hat{k}\times\frac{\partial \vec{V}_g}{\partial t} \quad [\because \hat{k}\times(\hat{k}\times\vec{V}) = -\vec{V}]$$

$$= -\frac{g}{f^2}\frac{\partial \nabla Z}{\partial t}$$

$$-f\hat{k} \times \frac{\partial \vec{V}_g}{\partial t} = g\,\nabla \frac{\partial Z}{\partial t} \tag{6-29}$$

因此

$$g\,\nabla \frac{\partial Z}{\partial t} = -f^2\,\vec{V}_{ag(i)} \tag{6-30}$$

$\frac{\partial}{\partial t}(\nabla Z)$ $-\nabla(\frac{\partial Z}{\partial t})$

此即表示 $\vec{V}_{ag(i)}$ 與等變高線的梯度成正比，而方向指向等高線下降的一側。(即指向低压)

（三）平流地轉偏差風分量（Advective Ageostrophic Wind）

氣塊平移時，因等高線的曲率不同，即不平行，故移行的軌跡與等高線間有差異，如圖6-6所示，

即当一気塊平移时，雖然在開始可達地轉(or gradient)平衡，但平移後，馬上進入另一种压力梯度力，使其失去原有之平衡，故気塊必須調節自己，使其再度達到新的平衡，這种調節之过程，即会產生加速度，因此產生了非地轉之分量來。

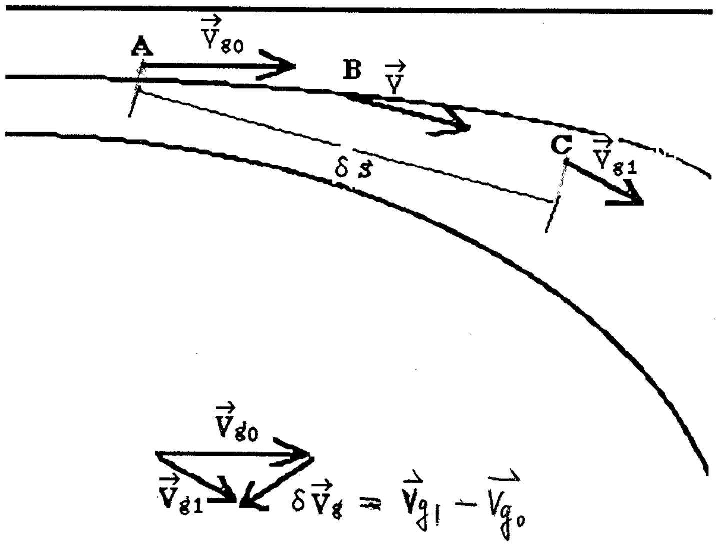

圖 6-6

因

$$-f\hat{k} \times \vec{V}_{ag(a)} = \vec{V} \cdot \nabla \vec{V}_g = |\,\vec{V}_B\,|\ \frac{\delta \vec{V}_g}{\delta s} \tag{6-31}$$

or $\vec{V}_{ag(a)} = \frac{|\vec{V}_B|}{f}\,\hat{k} \times \frac{\delta \vec{V}_g}{\delta s}$

故 $\vec{V}_{ag(a)}$ 與 $\delta\vec{V}_g$ 垂直，且在其左側。$\delta\vec{V}_g$ 有兩個分量，一垂直於 $\vec{V}_B$，它使風轉向，以趨向於平行(高的)等高線；另一在 $\vec{V}_B$ 的反(同)向，它使風速減小(增強)，在分流区(合流区)。~~以趨向分流等高線的梯度一致~~。因此，在分流處平流地轉偏差風分量偏向高壓；在合流處平流地轉偏差風分量偏向低壓。（如圖6-7）

$\because \vec{V}_{ag} = \frac{|\vec{V}_B|}{f}\hat{k}\times\frac{\delta\vec{V}_g}{\delta s}$

① 由 $\vec{V}_{g0}$ 及 $\vec{V}_{g1}$ 得 $\delta\vec{V}_g$

② 由 $\hat{k}\times\delta\vec{V}_g$ 得 $\vec{V}_{ag}$ #

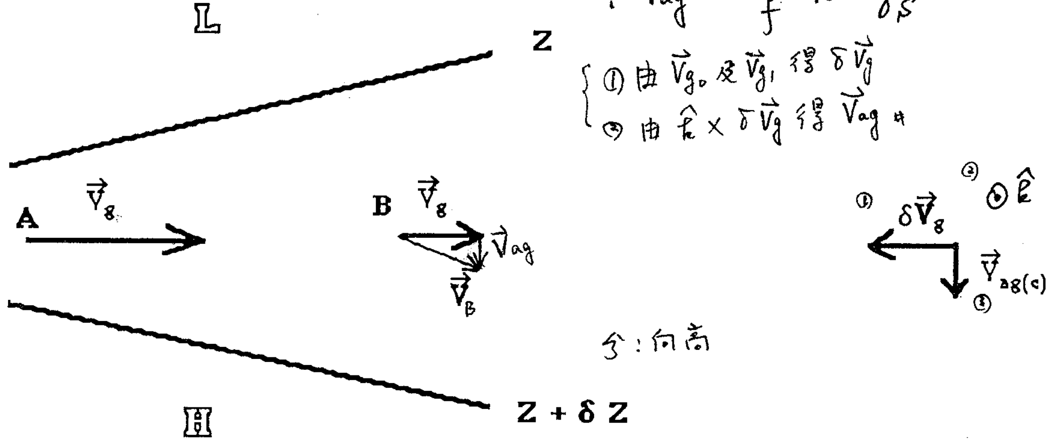

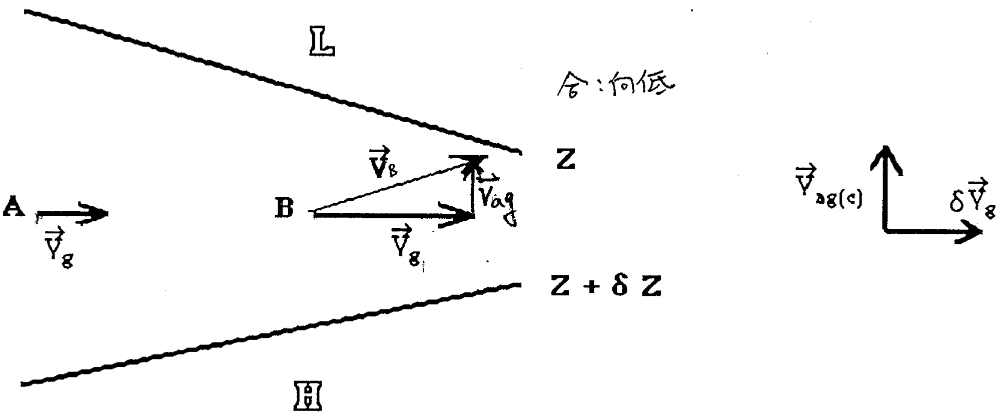

圖 6-7

⇒ 風速變小時(分流)，$\vec{V}_{ag}$ 指向右，∴ $\vec{V}$ 会向右偏，偏離低压。
風速變大时(合流)，$\vec{V}_{ag}$ 指向左，∴ $\vec{V}$ 会向左偏，偏向低压。

⇒ 均趨向於平行高的等高线。

(四) 對流地轉偏差風分量 (Convective Ageostrophic Wind)

因為

$$-f\hat{k} \times \vec{V}_{ag(c)} = \omega \frac{\partial \vec{V}_g}{\partial p} = \omega \frac{\delta \vec{V}_g}{\delta p} \Rightarrow \vec{V}_{ag(c)} = \frac{\overset{\ominus\uparrow}{\omega}}{\underset{\oplus\downarrow}{f}}\,\hat{k} \times \frac{\delta \vec{V}_g}{\delta p} \quad (6\text{-}32)$$

→熱力風

故在上升運動 ($\omega<0$) 處，$\omega\frac{\partial \vec{V}_g}{\partial p}$ 與 $\delta\vec{V}_g$ 同向，$\vec{V}_{ag(c)}$ 在 $\delta\vec{V}_g$ 的左側 (冷側)，即若氣流上升，則對流地轉偏差風與等溫線相交，且指向冷側；在下降運動 ($\omega>0$) 處，$\omega\frac{\partial \vec{V}_g}{\partial p}$ 與 $\delta\vec{V}_g$ 反向，$\vec{V}_{ag(c)}$ 在 $\delta\vec{V}_g$ 的右側 (暖側)，即若氣流下降，則對流地轉偏差風與等溫線相交，且指向暖側 (如圖 6-8)。

強烈的溫度水平梯度與垂直運動，將伴隨強盛的 $\vec{V}_{ag(c)}$。

$\frac{\delta \vec{V}_g}{\delta p}$

∴在垂直速度大之地區，如鋒面或山坡附近，及水平溫度梯度大之地區，如鋒面或海陸交界地區，均有強烈之此項效應。

{ 上升運動 V_{ag} 指向冷區
  下降運動 V_{ag} 指向暖區

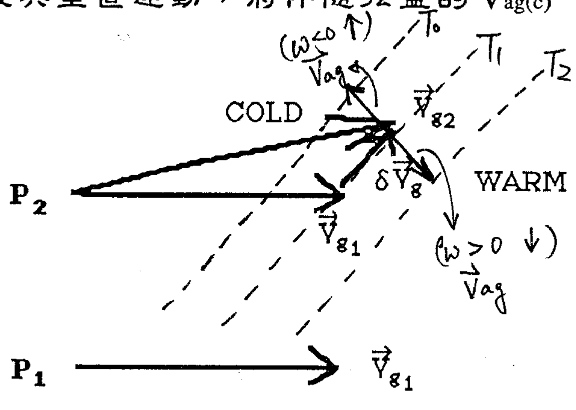

圖 6-8

(五) 加速度

$$-f\hat{k} \times \vec{V}_{ag(x)} = \frac{d\vec{V}_{ag}}{dt}$$

$$\frac{d\vec{V}_{ag}}{dt} = -f\hat{k} \times \vec{V}_{ag} \Rightarrow$$ ∴科氏加速力使其向右偏。 #

以上討論造成 V_{ag} 之各作用力。可是 V_{ag} 對大氣運動 (加速度) 的影響，還要再經過科氏力的作用，即 **$-f\,k \times dV_{ag}/dt$**。另外，摩擦力的討論要注意+/-號。

四、2 熱力風與厚度場分析

(熱力風之其他特性，請複習大動) C-5

C-2 熱力風和厚度場(溫度場)的分析.

由流体靜力平衡關係知，兩等壓面間之厚度正比此層大氣之平均溫度，

即 $\frac{\partial z}{\partial p} = -\frac{RT}{p}$.

而兩等壓面上地轉風之向量差，定义為這層大氣的熱力風，$\vec{V}_T$，向量，

即 $\vec{V}_T = \vec{V}_{g上層} - \vec{V}_{g下層}$

(由 $\vec{V}_g = -\frac{g}{f}\hat{k}\times\nabla_p z$，∴ $\frac{\partial \vec{V}_g}{\partial p} = -\frac{g}{f}\hat{k}\times\nabla_p\left(\frac{\partial z}{\partial p}\right) = \frac{R}{fp}\hat{k}\times\underbrace{\nabla_p(T)}_{水平溫度梯度}$)

∴熱力風之大小為：$V_T = \frac{g}{f}\left(\frac{\partial \Delta z}{\partial n}\right) = \frac{g}{f}\frac{\delta\Delta z}{\delta n}$.

因此，$\vec{V}_T$ 和 Δz 的關係就相當於 $\vec{V}_g$ 和 Z 之關係。∴亦可使用前面圖C-1查出不同緯度之相隣兩條等厚度線的距離，來判斷熱力風之大小。

而在正壓的區域，風速和氣流的形勢都不隨高度改變，即 $\frac{\partial \vec{V}_g}{\partial z} = 0$。

即垂直風切正比於水平溫度梯度。一般在中緯度地區有最大之 $\frac{\partial T}{\partial y}$，故其上層之 U_g 亦最強(噴流之位置)。另外在夏季，南亞地區之上空，∵青藏高原所致之加熱作用，使得此區之溫度分布北高南低($\frac{\partial T}{\partial y}$ 反向)，故此區之上方有東風噴流(而非西風)。∴噴流處 ∇T 較大；而鋒面處，∵∇T 較大，故上層有噴流。

*另外由冷平流時，風向隨高度增加是逆時針方向改變；而暖平流為順時針。故可用探空資料(風向)來判斷一系統是在移進或移出。

* 厚度場之變化和平均溫度之關係.

$\int\left[dz = -\frac{RT}{gp}dp\right] \Rightarrow z_2 - z_1 = \frac{R}{g}\bar{T}\ln\frac{P_1}{P_2}$

∴ $\left(\frac{\partial z}{\partial t}\right)_2 - \left(\frac{\partial z}{\partial t}\right)_1 = \frac{R}{g}\ln\frac{P_1}{P_2}\frac{\partial \bar{T}}{\partial t}$.

即兩等壓面間之厚度變化，$(z_2-z_1)/\Delta t$，趨勢只和其間之平均溫度變化趨勢成正比。若兩等壓面間之溫度不變，則此二等壓面之高度變化趨勢相等(厚度不變)

若其平均溫度增高，則會使等壓面向上抬升，且上層比下層抬升更高

降低，向下降落，且 - - - 降落更多。

∴溫度增高，$\frac{\partial \bar{T}}{\partial t} > 0$，為暖平流，則 $\frac{\partial z_2}{\partial t} > \frac{\partial z_1}{\partial t}$，∴即 Δz_2 比 Δz_1 大，上層上升更多，厚度變厚。

四、3 槽與脊隨高度的傾斜

C-3: 等壓面上脊(或H)、槽(或L)隨高度的傾斜.

可以由下列之觀點來討論:

(i) 大動之 2-layer model (§8-2) 或 tendency eq. (§6.3): 自己複習.

(ii) $\tan\psi$ 之討論 $\left(\frac{\delta z}{\delta s}\right)$

(iii)

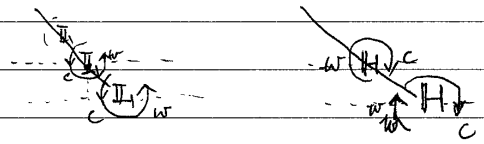

(iv) 更完整之討論 $\left(\frac{\delta z}{\delta s}\right)$

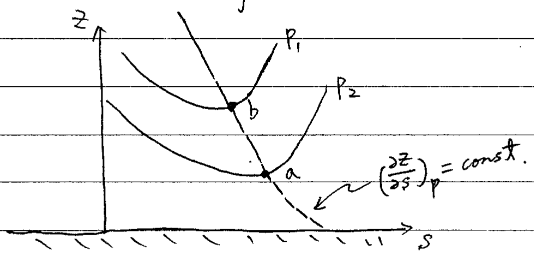

設 a 及 b 分別在等壓面 P_2 及 P_1 上, 且在這兩點上等壓面之斜率, $\left(\frac{\partial z}{\partial s}\right)_p$, 相等。我們要探討此天氣系統隨高度增加而傾斜的情形。

由流体靜力平衡: $\frac{\partial z}{\partial p} = -\frac{\alpha}{g}$ $\Rightarrow \delta z = -\frac{\alpha}{g}\delta p$

$\Rightarrow z_b - z_a = -\frac{\alpha}{g}\delta p \; ; \; \delta p = P_1 - P_2$.

又∵ $\left(\frac{\partial z}{\partial s}\right)$ 是 s 和 p 之函數,

$$\therefore \delta\left(\frac{\partial z}{\partial s}\right) = \frac{\partial}{\partial s}\left(\frac{\partial z}{\partial s}\right)\delta s + \frac{\partial}{\partial p}\left(\frac{\partial z}{\partial s}\right)\delta p = \frac{\partial^2 z}{\partial s^2}\delta s - \frac{\partial \alpha}{\partial s}\frac{\delta p}{g}$$

對兩等壓面上斜率相同之點而言:

$$\left(\frac{\partial z}{\partial s}\right)_b - \left(\frac{\partial z}{\partial s}\right)_a = 0 = \left(\frac{\partial^2 z}{\partial s^2}\right)\delta s - \left(\frac{\partial \alpha}{\partial s}\right)\frac{\delta p}{g}$$

$$\therefore \frac{\delta p}{\delta s} = g\,\frac{\left(\frac{\partial^2 z}{\partial s^2}\right)_p}{\left(\frac{\partial \alpha}{\partial s}\right)_p}$$, 由 $\delta p = -\frac{g}{\alpha}\delta z$

$$\Rightarrow \frac{\delta z}{\delta s} = -\frac{\left(\frac{\partial^2 z}{\partial s^2}\right)_p}{\frac{1}{\alpha}\left(\frac{\partial \alpha}{\partial s}\right)_p} = -\frac{\left(\frac{\partial^2 z}{\partial s^2}\right)_p}{\frac{1}{T}\left(\frac{\partial T}{\partial s}\right)_p} \quad \text{——} (*)$$

在等壓面上:

在槽(或L)處, $\left(\frac{\partial^2 z}{\partial s^2}\right) > 0$; 在脊處 $\left(\frac{\partial^2 z}{\partial s^2}\right) < 0$.

(分子表示系统(等高线)弯曲(曲率)的大小.

在式(*)中,分母表示斜压性的大小。在正压的状况下,$(\frac{\partial T}{\partial s})_p=0$,∴
脊(∝H)和槽(∝L)没有倾斜。
而在斜压性很强的地方,分母很大,∴$\frac{\delta z}{\delta s}$很小,
即系统随高度增加而倾斜得很厉害。

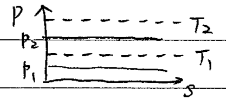

① 在$(\frac{\partial T}{\partial s})_p>0$时:
a: 在槽(∝L)处,$\frac{\delta z}{\delta s}<0$,则槽向$-s$(冷侧)倾斜
b. 在脊(∝H)处, 〃 >0,∴脊向$+s$(暖侧) 〃 〃

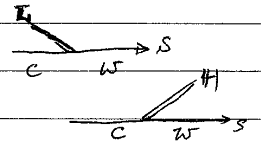

② 若$(\frac{\partial T}{\partial s})_p<0$,
a. 在槽处,$\frac{\delta z}{\delta s}>0$,则槽向$+s$(冷侧)倾斜
b. 在脊处,$\frac{\delta z}{\delta s}<0$,则脊向$-s$(暖侧) 〃 〃

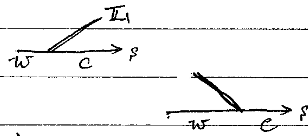

⇒ 在一般大气,∵$\frac{\delta z}{\delta s}<0$,∴脊向西倾斜(南北半球均同)
⇒ 综之,脊或高压中心随高度增大而向暖侧倾斜。而低压(槽)向冷侧倾斜。

*另外由公式(*)知,等压面之曲率,$\frac{\partial^2 z}{\partial s^2}$,越大(即等高线越弯曲),则$\frac{\delta z}{\delta s}$也越大,∴系统越垂直 ,倾斜越小。
反之,较平浅的天气系统,$\frac{\delta z}{\delta s}$越小,倾斜得越厉害, 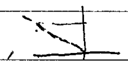

* 若L_1和L_2两圆形低压系统之等压面向上弯曲的曲率相同,但在L_2附近之温度梯度较大,则L_2之倾斜会较厉害(∵分母大,$\frac{\delta z}{\delta s}$小)

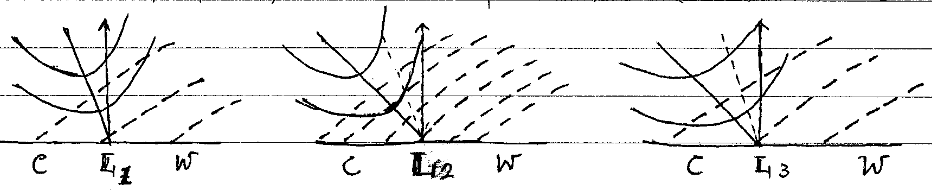

$(\frac{\partial^2 z}{\partial s^2})_1=(\frac{\partial^2 z}{\partial s^2})_2$,但$(\frac{\partial T}{\partial s})_1<(\frac{\partial T}{\partial s})_2$ $\quad$ $(\frac{\partial T}{\partial s})_1=(\frac{\partial T}{\partial s})_3$ 但$(\frac{\partial^2 z}{\partial s^2})_1>(\frac{\partial^2 z}{\partial s^2})_3$

∴$(\frac{\delta z}{\delta s})_2<(\frac{\delta z}{\delta s})_1$ $\quad$ ∴$(\frac{\delta z}{\delta s})_3<(\frac{\delta z}{\delta s})_1$

另外若L_1和L_3附近之温度梯度相同,但L_1之等压面向上弯曲较厉害(等压线较紧集),则L_3随高度向冷侧倾斜较厉害

* 总之:一圆形气旋(反气旋)中心随高度递增会向冷(暖)侧倾斜。其倾斜的程度(δs之大小)和(水平)温度梯度成正比;而与等压面向上(下)弯曲之曲率($\frac{\partial^2 z}{\partial s^2}$)成反比。 $(\frac{\partial T}{\partial s})$

斜壓性的增強是中緯度天氣系統生成與加強的根本原因，其能量的來源就是「可用位能」，可由下列幾個因子來判斷：

1. **可用位能**的增加，即暖空氣爬到冷空氣上方，或冷空氣鑽到暖空氣下方；
   主要的原因：空氣的冷暖平流。東亞主槽/主脊 系統的加強或移入，或上層渦度的平流等。
2. 天氣圖（斜溫圖）分析上，主要之現象（特徵）為：，
   a. 水平向等高線與等溫線的夾角大小（即不平行），即高度槽與溫度槽的相位差(90°)。
   b. 力管項的大小，$(\frac{\partial \rho}{\partial x}\frac{\partial P}{\partial y}-\frac{\partial \rho}{\partial y}\frac{\partial P}{\partial x}) \quad or \quad (\nabla\alpha\times\nabla P)\bullet\hat{k}$；在垂直向亦有力管項。
   c.. 系統在垂直方向的向西傾斜。
   d. 有熱力風，水平溫度梯度或垂直風切，即水平溫度平流。
   e. 或分析水平的輻合及輻散，及垂直速度。

with increasing distance from the center, gradients can be larger.

From Eqs (4) and (5) above it follows that *the maximum anticyclonic gradient wind is precisely twice the geostrophic wind for that contour gradient*, or c_{gr} max $= 2c_g$. This is the maximum *equilibrium* wind in anticyclonically curved flow; it does not imply that actual winds cannot exceed it.

The quadratic equation for cyclonic gradient wind is solved in a similar manner:

$$c_{gr} = -fR/2 + \sqrt{[R^2f^2/4 + 980R(\partial Z/\partial n)_p]}\,. \quad \text{(cyclonic)} \qquad (6)$$

The quantity beneath the radical is always positive, and its square root is greater than $fR/2$. In this equation there is no restriction on magnitude of pressure gradient to maintain real roots of the quadratic. A useful interpretation is that cyclones can have larger gradients than anticyclones, and such is usually the case. On the pressure charts illustrated observe the asymmetry in distribution of gradients between HIGHs and LOWs at all levels. In fact, the maximum pressure slope is usually somewhat nearer the cyclone center than the center of the adjacent anticyclone. Another verification is that intense tropical storms are observed while analogous anticyclonic circulations are not found.

It is usually assumed in practice that the effect of surface friction decreases rapidly with height, and at levels 500 meters or 2000 feet above ground the wind should attain balance with the pressure field. Such a level can be taken as the *gradient level*. As an aid in sea-level pressure analysis, these winds are often entered on the surface chart. These are called "gradient winds"; more properly, "gradient-level winds." They are not necessarily in gradient balance according to the gradient-wind equations given above.

7.23. *Accelerations with unbalanced forces.*—The principal forces governing motions in the atmosphere are the pressure, the Coriolis, and the frictional forces. The horizontal acceleration acting on a parcel of air can be considered the unbalanced residual of these forces per unit mass. That is,

$$d\mathfrak{C}/dt = f * (\mathfrak{C} - \mathfrak{C}_g) + \mathbf{F}\,. \qquad (1)$$

$(\mathfrak{C} - \mathfrak{C}_g)$ is always the vector difference between actual and geostrophic wind. This difference is ageostrophic wind, denoted $\mathfrak{C}'$ (Fig. 7.04*b*). From Eq (1) it follows that the net acceleration is the vector difference

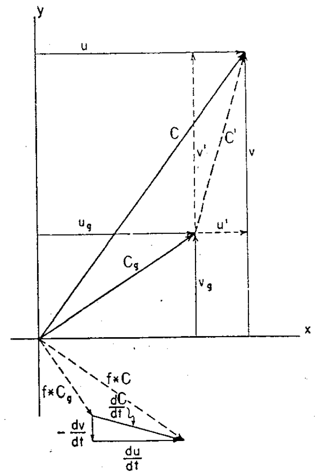

FIG. 7.231.—Graphical relation of acceleration and ageostrophic wind in frictionless motion.

between actual Coriolis force $f * \mathfrak{C}$ and that Coriolis force $f * \mathfrak{C}_g$ for geostrophic wind, when $\mathbf{F} \approx 0$. (It is $d\mathfrak{C}/dt - \mathbf{F}$ when friction is included.) This difference is shown as $d\mathfrak{C}/dt$ in the lower part of Figure 7.231. Notice that it is perpendicular to the ageostrophic wind $\mathfrak{C}'$ and directed to the right of $\mathfrak{C}'$. In absence of friction, *the acceleration is actually the Coriolis force per unit mass for the ageostrophic wind.*

From the illustration above it is evident that, if $\mathfrak{C}$ has geostrophic direction but $c > c_g$, then $\mathfrak{C}'$ is along the wind direction, and acceleration is to the right of the wind. Thus, *supergeostrophic winds are accelerated to the right of the geostrophic wind.* Anticyclonically curved flow in gradient conditions is one special case. If $c < c_g$ but both are of same direction, acceleration is to the left of the wind. Therefore, *subgeostrophic winds are accelerated to the left of the geostrophic wind*, and gradient cyclonic flow is one special case of that type.

Acceleration may be given also in terms of the coordinate components of wind. It is seen from further examination of Figure 7.231 that

$$du/dt - F_x = fv' = f(v - v_g)\,, \qquad (1a)$$

and

$$dv/dt - F_y = -fu' = -f(u - u_g)\,. \qquad (1b)$$

From the three equations above, the magnitude of acceleration can be determined relative to the ageostrophic wind. Since f is of magnitude 10^{-4} sec^{-1}, acceleration is about 1/10,000 as large in the same system of units as ageostrophic speed in middle latitudes. The change of wind speed by an acceleration acting over a long time may be large. In only 3 hours (10,800 seconds) a constant acceleration gives change of wind speed about equal to the initial ageostrophic wind.

It is of interest to investigate the factors giving accelerations to motion and consequently departures from geostrophic balance, for, if we are to employ the geostrophic and gradient wind equations at all, we should be aware of some conditions with departures. If actual wind is expressed as the sum of geostrophic wind and the ageostrophic component: $\mathfrak{C} = \mathfrak{C}_g + \mathfrak{C}'$; $u = u_g + u'$; $v = v_g + v'$. The total time derivatives of $\mathfrak{C}$, u, and v are $d\mathfrak{C}/dt = d\mathfrak{C}_g/dt + d\mathfrak{C}'/dt$; $du/dt = du_g/dt + du'/dt$; $dv/dt = dv_g/dt + dv'/dt$.

It is now seen that acceleration can be examined in two parts, viz., the contribution by geostrophic acceleration and that by ageostrophic acceleration. We shall not investigate the latter. Since geostrophic acceleration can be described adequately in terms of pressure and isallobaric[24] fields, it is worth while finding as much as possible concerning this contribution to total acceleration.

We may transform the geostrophic part of the equations above by use of the differential operator

$$\frac{d}{dt} = \frac{\partial}{\partial t} + \mathfrak{C}\cdot\nabla_h + w\frac{\partial}{\partial z} = \frac{\partial}{\partial t} + u\frac{\partial}{\partial x} + v\frac{\partial}{\partial y} + w\frac{\partial}{\partial z}\,.$$

Then, by Eqs (1), (1a), and (1b),

$$d\mathfrak{C}/dt - \mathbf{F} = f * \mathfrak{C}' = \partial\mathfrak{C}_g/\partial t + \mathfrak{C}\cdot\nabla_h\mathfrak{C}_g + w(\partial\mathfrak{C}_g/\partial z) + d\mathfrak{C}'/dt - \mathbf{F}\,, \qquad (2)$$

$$du/dt - F_x = fv' = \partial u_g/\partial t + \mathfrak{C}\cdot\nabla_h u_g + w(\partial u_g/\partial z) + du'/dt - F_x\,, \qquad (2a)$$

$$dv/dt - F_y = -fu' = \partial v_g/\partial t + \mathfrak{C}\cdot\nabla_h v_g + w(\partial v_g/\partial z) + dv'/dt - F_y\,. \qquad (2b)$$

If the last two equations are divided by f and $-f$, respectively,

$$v' = \frac{1}{f}\frac{\partial u_g}{\partial t} + \frac{u}{f}\frac{\partial u_g}{\partial x} + \frac{v}{f}\frac{\partial u_g}{\partial y} + \frac{w}{f}\frac{\partial u_g}{\partial z} - \frac{F_x}{f} + \frac{1}{f}\frac{du'}{dt}\,, \qquad (3a)$$

$$u' = -\frac{1}{f}\frac{\partial v_g}{\partial t} - \frac{u}{f}\frac{\partial v_g}{\partial x} - \frac{v}{f}\frac{\partial v_g}{\partial y} - \frac{w}{f}\frac{\partial v_g}{\partial z} + \frac{F_y}{f} - \frac{1}{f}\frac{dv'}{dt}\,. \qquad (3b)$$

A similar expression holds for resultant ageostrophic wind $\mathfrak{C}'$. Obviously, these are not valid where $f = 0$.

Accelerations $\partial u_g/\partial t$ and $\partial v_g/\partial t$ comprise the *isallobaric acceleration* $\partial\mathfrak{C}_g/\partial t$ to geo-

24. Pressure change.

四、3 補充資料-1

(Saucier, W.J., 1965: Principles of Meteorological Analysis. 438pp) strophic wind, and, when divided by the Coriolis parameter, they give the *isallobaric wind* $\mathfrak{C}'_i$, which is that *part* of ageostrophic wind related to isallobaric acceleration. The terms $(u\partial u_g/\partial x + v\partial u_g/\partial y)$ and $(u\partial v_g/\partial x + v\partial v_g/\partial y)$ comprise the (horizontal) *advective acceleration* to geostrophic wind, $\mathfrak{C}\cdot\nabla_h\mathfrak{C}_g$. The corresponding quantities in the right sides of Eqs (3a) and (3b) give the *advective ageostrophic* wind $\mathfrak{C}'_a$. Next, $w(\partial u_g/\partial z)$ and $w(\partial v_g/\partial z)$ are the components of geostrophic acceleration due to vertical motion. As expressed in the last equations, those give the *convective ageostrophic wind* $\mathfrak{C}'_c$. Next are the frictional accelerations, which contribute the *antitriptic wind* $\mathfrak{C}'_F$. Finally, as seen by Eq (2) the ageostrophic acceleration also contributes to the net ageostrophic wind.

The resultant ageostrophic wind is the vector sum of all contributions:

$$\mathfrak{C}' = \mathfrak{C}'_i + \mathfrak{C}'_a + \mathfrak{C}'_c + \mathfrak{C}'_F + X ,$$

where X denotes ageostrophic wind related to ageostrophic acceleration. If that term is dropped (not suggesting it is small), we have

$$\mathfrak{C}' = \mathfrak{C}'_i + \mathfrak{C}'_a + \mathfrak{C}'_c + \mathfrak{C}'_F ; \quad (4)$$

$$u' = u'_i + u'_a + u'_c + u'_F ; \quad (4a)$$

$$v' = v'_i + v'_a + v'_c + v'_F . \quad (4b)$$

It will be remembered henceforth that the resultant ageostrophic wind being described is not the true resultant, since a term is omitted. However, valuable information can be obtained from the simplified form, and the equations we now have are more complete than presently considered in practice.

a) Antitriptic wind.—The most obvious departure from geostrophic balance is that due to friction with the earth's surface. The frictional stress between moving air and the earth first may be viewed as retardation ($\mathbf{F}_g$ in Fig. 7.232) acting opposite to the geostrophic wind. This decreases air motion, thus decreasing the Coriolis force. There results an acceleration toward lower pressure, as the pressure force is not affected directly, and the air develops a component of motion across contours (isobars) toward lower pressure. In the final adjusted state the wind is less than geostrophic and directed to the left of $\mathfrak{C}_g$ (northern hemisphere). In this state the frictional force $\mathbf{F}$, the Coriolis force $f * \mathfrak{C}$, and the pressure force are in equilibrium. Observe that

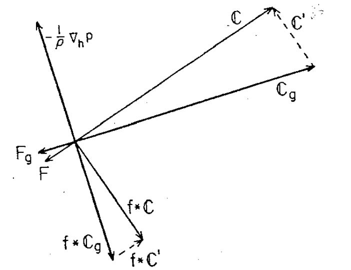

FIG. 7.232.—The effect of friction on geostrophic balance. (Shown here is a state of equilibrium between pressure, Coriolis, and frictional forces.)

$f * \mathfrak{C}' = -\mathbf{F}$, which is Eq (2) when $\mathfrak{C}'_i + \mathfrak{C}'_a + \mathfrak{C}'_c = 0$. In this condition $\mathfrak{C}'$ and $\mathfrak{C}$ are perpendicular, and therefore $c = c_g \cos \delta$, if δ is the angle between $\mathfrak{C}$ and the contours (isobars). This departure at the surface is a complicated function of wind distribution, surface roughness, and static stability in the friction layer. The effect of surface friction is shown clearly by comparing the winds in Figures 9.02*ab* with the gradient-level winds in Figure 7.03*h*.

b) Isallobaric wind.—The definition of isallobaric wind found above was first given by Brunt and Douglas,[25] who suggested that with large isallobaric gradients the isallobaric wind could account for the principal ageostrophic flow.

25. D. Brunt and C. K. M. Douglas, "The Modification of Strophic Balance for Changing Pressure Distribution, and Its Effect on Rainfall," *Memoirs of the Royal Meteorological Society*, Vol. III, No. 22 (1928).

Figure 7.233 gives the isobaric topography at an initial time (heavy solid lines), the topography after time δt (heavy dashed lines), and the isopleths (isallohypses, isallobars) of net change. At the right are the initial geostrophic wind $\mathfrak{C}_{g_0}$, final geostrophic wind $\mathfrak{C}_{g_1}$, and change $\delta\mathfrak{C}_g$ for point A. Vector $\delta\mathfrak{C}_g$ parallels isallobars, and its magnitude is proportional to the isallobaric gradient.

The effect of the isallobaric field is given by the first term on the right of Eqs (2). A part of $d\mathfrak{C}/dt$ (and a corresponding part of $\mathfrak{C}'$) is due to this local variation of geostrophic wind. We denote this contribution by

$$(d\mathfrak{C}/dt)_i = f * \mathfrak{C}'_i = \partial\mathfrak{C}_g/\partial t . \quad (5)$$

For convenience, only the first of Eqs (2) will be used.[26] The quantity $\partial\mathfrak{C}_g/\partial t$ is approximated by $\delta\mathfrak{C}_g/\delta t$. Accordingly, from Eq (5), $(d\mathfrak{C}/dt)_i\delta t = \delta\mathfrak{C}_g$. Isallobaric acceleration is *along* $\delta\mathfrak{C}_g$, with larger falling tendencies to the left (Fig. 7.233).

Eq (5) shows that an isallobaric acceleration corresponds to isallobaric wind $\mathfrak{C}'_i$ directed 90° to the left. Isallobaric wind then must be *directly proportional to and directed along the isallobaric descendant.* This may be shown also by differentiating the geostrophic equation $f * \mathfrak{C}_g = 980\ (\nabla Z)_p$ with respect to time; that is, $f * \partial\mathfrak{C}_g/\partial t = 980\ \nabla(\partial Z/\partial t)_p$. But from Eq (5), $f * (\partial\mathfrak{C}_g/\partial t) = f * (f * \mathfrak{C}'_i) = -f^2\mathfrak{C}'_i$, or $\mathfrak{C}'_i$ is directed 180° from the isallobaric ascendant $\nabla(\partial Z/\partial t)_p$. Then

$$\mathfrak{C}'_i = -(980/f^2)[\nabla(\partial Z/\partial t)_p] ,$$

or

$$c'_i = (980/f^2)[\partial(\partial Z/\partial t)_p/\partial n] . \quad (6)$$

Direction n is along the isallobaric ascendant. Thus, if isallobars are west-east with larger rises south, isallobaric wind is northward with speed proportional to the magnitude of the isallobaric gradient.

The isallobaric wind speed may be evaluated directly from the tendency field by the scalar form of Eq (6). For example, where $f = 10^{-4}$ sec^{-1} and the tendency gradient is 10 gpft per hour per 100 km (a rather large value), isallobaric wind is about 8 m sec^{-1}.

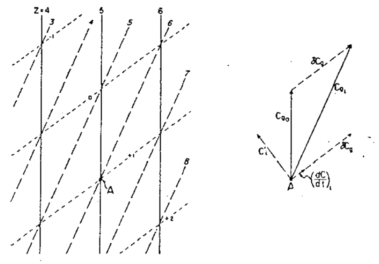

FIG. 7.233.—The isallobaric wind in relation to the isallobaric pattern.

The validity of the isallobaric wind measured from a pattern of pressure change is dependent on how well the field of integrated change during the period indicates the field of instantaneous tendency. In the moving wave pattern in Figure 7.144 the true isallobaric winds would be directed toward the inflection point in the current center in advance of the trough and away from the opposite inflection point. The field of isallobaric wind deduced from the change patterns in the drawing gives quite an erroneous picture. In general, the longer the time interval for pressure change, the greater is the discrepancy between indicated and true isallobaric wind fields.

The degree to which the isallobaric wind $\mathfrak{C}'_i$ approximates total ageostrophic wind $\mathfrak{C}'$ depends on the contribution by the remaining terms[27] on the right side of Eq (2). It is

26. For slightly different derivations using coordinate components refer to B. Haurwitz, *Dynamic Meteorology* (New York: McGraw-Hill Book Co., 1941), pp. 155–59, and E. W. Hewson and R. W. Longley, *Meteorology: Theoretical and Applied* (New York: John Wiley & Sons, 1944), pp. 128–30.

27. A more detailed discussion of the relative importance of the isallobaric contribution is given by B. Haurwitz, "On the Relation between the Wind Field and Pressure Changes," *Journal of Meteorology*, III (1946), 95–99.

apparent that even with strong isallobaric wind the ageostrophic wind may be zero or even opposite to the isallobaric wind. Thus *it is improper to attribute existing ageostrophic winds only to the isallobaric pattern until all other factors have been accounted for.* (For gradient winds in an isallobaric field the requirement is that the sum of all terms on the right of Eq [2] equals $d\mathfrak{C}_{gr}/dt$.)

c) Advective ageostrophic wind.—As an air parcel moves horizontally, the pressure pattern usually varies along its trajectory. This is true even if the pressure field is steady, for contours are not straight or uniformly curved and not parallel over large distances. Thus, an air parcel which at one instant is in geostrophic (or gradient) balance soon may find itself in a different pressure field. To readjust itself, the parcel is subjected to acceleration and thus develops an ageostrophic component. From this viewpoint alone it is easy to see that geostrophic or gradient wind is rarely precisely fulfilled on synoptic pressure charts.

The effect of horizontal variations in the pressure pattern on accelerations is given by $\mathfrak{C}\cdot\nabla_h\mathfrak{C}_g$ in Eq (2). We may write $\mathfrak{C}\cdot\nabla_h\mathfrak{C}_g = c(\partial\mathfrak{C}_g/\partial s)$, where s is distance downwind through the point in question, and $\partial\mathfrak{C}_g/\partial s$ is the variation of vector geostrophic wind in that direction (Fig. 7.234). If acceleration due to this effect is $(d\mathfrak{C}/dt)_a$ and the corresponding ageostrophic wind is $\mathfrak{C}_a'$, then

$$(d\mathfrak{C}/dt)_a = f * \mathfrak{C}_a' = c(\partial\mathfrak{C}_g/\partial s)\,. \quad (7)$$

The advective contribution is illustrated graphically[28] in Figure 7.234. Geostrophic winds are measured from the pressure pattern at points δs apart and equidistant from b. Vector $\delta\mathfrak{C}_g$ is the difference in geostrophic winds upstream and downstream from b. Dividing $\delta\mathfrak{C}_g$ by δs approximates $\partial\mathfrak{C}_g/\partial s$, which lies along $\delta\mathfrak{C}_g$. From Eq (7) the acceleration is along $\delta\mathfrak{C}_g$ and directly proportional to wind speed as well as to the magnitude of $\delta\mathfrak{C}_g/\delta s$. The ageostrophic wind is 90° to the left of $\delta\mathfrak{C}_g$. Notice in this example that the acceleration has a component to the right of the wind, indicating clockwise turning of wind in partial agreement with the contour pattern, and also a component opposite to the wind $\mathfrak{C}$, implying retarded motion in agreement with the divergence of contours.

If $\partial\mathfrak{C}_g/\partial s$ is normal to the actual wind $\mathfrak{C}$, then the ageostrophic wind lies along the

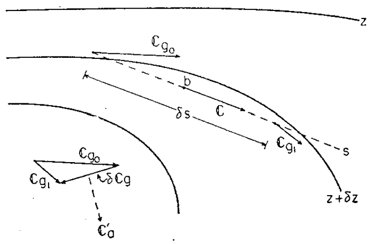

Fig. 7.234

actual wind, the acceleration is centripetal, and the motion is parallel to the contours. This is a statement of the gradient-wind condition for a steady pressure field and horizontal motion. In fact, one can show that $\mathfrak{C}\cdot\nabla_h\mathfrak{C}$ is the cyclostrophic acceleration in the gradient-wind equation with the same assumptions. By neglecting this advective term in the acceleration, the gradient-wind correction is being neglected.

Figure 7.235 gives simple illustrations of the advective effect on ageostrophic winds. Shown here are the three pressure patterns possible with straight contours, but deductions are also applicable to curved contours. For each case we might assume the wind is geostrophic initially at a. In the first diagram, as the air moves from a to b, it experiences no acceleration due to space variation of the pressure field; this wind remains

28. This can be shown also by superimposing the pressure patterns at two points in a manner similar to Figure 7.233.

geostrophic. In the second the contours diverge downwind, the motion is retarded, and ageostrophic wind is to the right. In the last diagram the effect is opposite.

To show the approximate value of ageo-

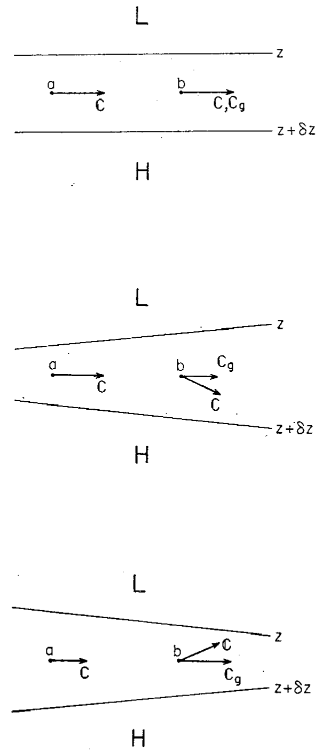

Fig. 7.235.—The departure of actual wind from geostrophic due to changing pressure gradients in the direction of motion.

strophic wind resulting from the advective contribution, average values may be substituted into Eq (7). If $f = 10^{-4}$ sec^{-1}, wind speed is 10 m sec^{-1}, and geostrophic wind from the same direction varies 5 m sec^{-1} per 100 km along the wind, then $c_a' \simeq 5$ m sec^{-1}. This is the same order of magnitude as the isallobaric wind. With stronger winds this effect can be more important than the isallobaric influence.

Deductions made on the basis of Figure 7.235 may be formulated into a set of general rules applicable to most synoptic patterns of pressure and wind. *If air moves into a weaker pressure field, it is deflected to the right of the contours and its motion retarded, and, if air moves into a stronger pressure field, it is deflected to the left of the contours and its motion accelerated*, provided its motion is in reasonable agreement with the pressure pattern initially. These rules exclude contributions by other terms in Eq (2), and they may not be strictly valid in certain critical conditions of curved flow or curved contours.[29]

There is frequent empirical evidence of the general rules given above for advective accelerations to the wind, not so much at the surface, where it is difficult to separate effects of friction, but at levels sufficiently higher, where there are still plentiful wind data. In Figure 7.03*g* there are several supergradient winds in the south central United States where contours diverge rapidly downstream. Here the winds differ less from those upstream than consistent with the widening of contour channels. Still farther upstream west of Lake Winnipeg, where contours converge downstream, it appears that winds are subgradient in having come from the weak pressure ridge over western Canada.

d) Convective ageostrophic wind.—The discussion above was devoted to varying pressure fields for horizontal air motion only; horizontal accelerations due to vertical displacements from one pressure pattern to another must be considered also. The vertical component of motion is ordinarily very

29. It is possible for the air to be accelerated while moving into a weaker pressure field if the contours vary in curvature sufficiently; in this case, supergradient winds toward lower pressure.

small relative to the horizontal component, but vertical variation of pressure patterns is usually so many times greater than horizontal variation that accelerations resulting from vertical displacements are not always negligible in comparison.

From Eq (2) acceleration $(d\mathfrak{C}/dt)_c$ due to vertical displacement may be represented in the same form as Eq (7). Thus,

$$(d\mathfrak{C}/dt)_c = f * \mathfrak{C}_c' = w(\partial\mathfrak{C}_g/\partial z)\ . \quad (8)$$

Vector $\partial\mathfrak{C}_g/\partial z$ is the variation of geostrophic wind with height; it is the thermal wind in a thin layer divided by the depth.

In Figure 7.07 are given the vector geostrophic winds $\mathfrak{C}_{g1}$ at lower level z_1 and $\mathfrak{C}_{g2}$ at upper level z_2; the difference, $\Delta\mathfrak{C}_g$, divided by the layer depth is the approximation to $\partial\mathfrak{C}_g/\partial z$, which has the direction of $\Delta\mathfrak{C}_g$. For upward motion $w > 0$, and from Eq (8) acceleration $(d\mathfrak{C}/dt)_c$ is along $\Delta\mathfrak{C}_g$. The related ageostrophic wind is to the left of $\Delta\mathfrak{C}_g$. Thus, *ageostrophic wind $\mathfrak{C}_c'$ blows across isotherms toward colder air in upward motion; it is directed toward warmer air in downward motion.*

As an example, consider that geostrophic wind is from west at 700 mb and zero at 850 mb. The thermal wind in the layer is then from west. With ascent the air is accelerated eastward and has ageostrophic component from south. For descent the resulting ageostrophic component is from north. If the air rises rapidly, it arrives at 700 mb with actual motion from south of west.

In barotropic regions vertical displacements should give no horizontal accelerations to the velocity. Large horizontal temperature gradients are favorable for development of ageostrophic winds by vertical displacements and can give an appreciable contribution to the total ageostrophic wind. For $f = 10^{-4}$ sec^{-1} and $\partial\mathfrak{C}_g/\partial z = 10$ m sec^{-1} per kilometer (horizontal temperature gradient about 3° C/100 km), Eq (8) gives speed for $\mathfrak{C}_c'$ 1 m sec^{-1} for each 1 cm sec^{-1} of vertical velocity. That vertical velocity may be considered an average absolute value in large-scale atmospheric motion.[30] The above result for convective ageostrophic wind might appear small in comparison with the others, but there are frequent situations in which vertical velocity and thermal wind are both larger than the values used. In effect, this contribution easily can be as important as those above.

There are several areas in the 850-mb chart for 1 March 1950 through which large vertical velocities might be expected. Along the east coast of the United States north of the Florida peninsula upward motion is evidenced by high humidities aloft and precipitation. Unfortunately, for the same reason wind data are few. Because gradient-level winds are from southwest and the 850-mb geostrophic winds are slightly stronger from west, implying ageostrophic motion northeastward with ascent, 850-mb winds in this area should cross contours to the left. Another region of suspected ascent in the lower atmosphere is the west coast of North America north of 45° latitude. Here the winds in the vicinity of 850 mb are accelerated not just by upward displacement but also by forced flow toward lower pressure induced by terrain.

Over the south central United States strong subsidence is occurring just behind the cold front. Winds at 700 mb are from west or west-northwest with average speeds about 50 knots. The 850-mb chart shows, below this, geostrophic winds from northwest with smaller speeds. In descending to this level, the air is accelerated to southwest (ageostrophic wind from northwest), resulting in northwesterly winds supergeostrophic for that level. In this area at 850 mb

30. H. A. Panofsky, "Large-Scale Vertical Velocity and Divergence," in American Meteorological Society, *Compendium of Meteorology*, pp. 639–46.

the winds are stronger than geostrophic conceivably because of ageostrophic wind by subsidence and by transport horizontally into a field of diverging contours.

Although vertical velocities must terminate at the earth's surface (where it is level), ageostrophic winds due to strong subsidence can be felt even in surface winds if there is sufficient turbulent mixing to carry the effect downward through the friction layer. Accelerations and ageostrophic winds at the surface developed through subsidence should be particularly evident just behind cold fronts, where thermal wind is large and where lack of stability in the friction layer is conducive to turbulent mixing. This could be a major contribution to ageostrophic flow behind the cold front over Texas in Figures 9.02*ab*.

7.24. *Stability for horizontal and vertical displacements.*—In Chapter 3 a discussion of atmospheric stability was given for vertical displacements only. Stability for horizontal and arbitrary displacements deserves similar treatment, but unfortunately little has been done with that phase of the subject. What appears below is a modified version of Van Meigham's summary in the *Compendium of Meteorology* (1951).

Consider a geostrophic current (Fig. 7.24) of invariant wind direction α in a small region of space. To simplify the discussion, the xy-plane is oriented with x-axis downwind, instead of by local grid coordinates on the earth. In this scheme $v_g = \partial v_g/\partial x = \partial v_g/\partial y = \partial v_g/\partial z = 0$, assuming also there is no temperature gradient downwind. Furthermore, if $U_0 = (u_g)_0$ is geostrophic velocity at any point A_0 along x, geostrophic velocity $U_A = (u_g)_A$ at A located a small distance $(\delta y, \delta z)$ transverse to the x-axis is

$$U_A = U_0 + (\partial u_g/\partial y)_0\,\delta y + (\partial u_g/\partial z)_0\,\delta z\ . \quad (1)$$

In such a coordinate system the equations of motion are

$$du/dt = 2\omega w \cos\phi \sin\alpha + 2\omega v \sin\phi - \alpha(\partial p/\partial x)\ , \quad (2a)$$

$$dv/dt = -2\omega u \sin\phi - 2\omega w \cos\phi \times \cos\alpha - \alpha(\partial p/\partial y)\ , \quad (2b)$$

$$dw/dt = -2\omega u \cos\phi \sin\alpha + 2\omega v \times \cos\phi \cos\alpha - \alpha(\partial p/\partial z) - g\ , \quad (2c)$$

if extraneous forces F_x, F_y, F_z are neglected. In the subsequent discussion we use the

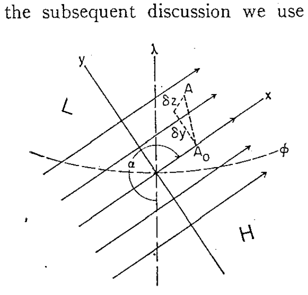

Fig. 7.24

notations: $2\omega \sin\phi = f$, $2\omega\cos\phi\sin\alpha = B$, and $2\omega\cos\phi\cos\alpha = C$.

Now suppose a parcel of unit mass at A_0 is given transverse velocity v_1, w_1 by some temporary impulse; after a small interval dt the parcel occupies position A, which constitutes displacement δy, δz from A_0. At this new position the parcel is assumed to have the pressure of its environment, and its component of acceleration along x is $(du/dt)_A = Bw_1 + fv_1$. Upon integration,

$$u_A = B\delta z + f\delta y + U_0\ . \quad (3)$$

This velocity component *relative* to geostrophic flow at A is $u_1 = u_A - U_A$; by substitution of U_0 from Eq (1) into Eq (3),

$$u_1 = (f - \partial u_g/\partial y)\delta y + (B - \partial u_g/\partial z)\delta z\ . \quad (4)$$

We now can determine the transverse horizontal component dv/dt of the parcel's acceleration at A. From Eqs (2b) and (4)

$$(dv/dt)_A = -f(f - \partial u_g/\partial y)\delta y - f(B - \partial u_g/\partial z)\delta z - Cw_1 \,. \quad (5)$$

Vertical acceleration resulting from displacement of the parcel is

$$(dw/dt)_A = -Bu_A + Cv_1 - c_p\,\theta_0 \times [\partial(p/1000)^\kappa/\partial z] - g \,. \quad (6)$$

The next-to-last term on the right is merely the vertical pressure force expressed in potential temperature. We now introduce the assumption that transverse displacement of the parcel is dry adiabatic. Necessity for this assumption[31] is apparent from definition of static stability in Chapter 3.

Vertical acceleration of the *undisturbed* geostrophic motion at A is

$$dw/dt \doteq 0 = -BU_A - c_p\theta_A\frac{\partial}{\partial z}\left(\frac{p}{1000}\right)^\kappa - g \,. \quad (7)$$

Upon subtracting Eq (7) from Eq (6) and substituting for u_1 from Eq (4),

$$(dw/dt)_A = -B(f - \partial u_g/\partial y)\,\delta y - B(B - \partial u_g/\partial z)\,\delta z + B\,v_1 - c_p(\theta_0 - \theta_A)\frac{\partial}{\partial z}\left(\frac{p}{1000}\right)^\kappa .$$

Now $\theta_0 - \theta_A$ may be expressed in terms of δy and δz by $\theta_0 - \theta_A = -(\partial\theta/\partial y)\delta y - (\partial\theta/\partial z)\delta z$. Also,

$$\frac{\partial}{\partial z}\left(\frac{p}{1000}\right)^\kappa = \frac{1}{c_p\rho\theta}\frac{\partial p}{\partial z} \simeq -\frac{g}{c_p\theta} .$$

31. The assumption of adiabatic displacement should have been made in deriving Eq (5) for a more complete expression for $(dv/dt)_A$, which is obtained from Eq (5) by adding

$$\alpha\frac{\partial p}{\partial y}\left(\frac{1}{\theta}\frac{\partial\theta}{\partial y}\,\delta y + \frac{1}{\theta}\frac{\partial\theta}{\partial z}\,\delta z\right)$$

to the right side of the equation, constituting negligible correction for horizontal displacement.

Therefore,

$$(dw/dt)_A = -B(f - \partial u_g/\partial y)\delta y - B(B - \partial u_g/\partial z)\delta z + Bv_1 - (g/\theta) \times (\partial\theta/\partial y)\delta y - (g/\theta)(\partial\theta/\partial z)\delta z \,. \quad (8)$$

Eqs (5) and (8) express the transverse horizontal and vertical accelerations resulting from displacement (δy, δz) with perturbation velocity v_1, w_1 of a parcel initially moving with geostrophic wind. The state of stability or instability exists according as the accelerations tend to return the parcel to the reference axis (x-axis) or carry it farther away. For each of these equations there has come to be defined a corresponding type of stability. If the displacement is vertical only, we speak of *static* stability. With displacements in the horizontal only, we have come to associate horizontal or *inertia* stability.

Static stability can be found directly from Eq (8). If $v_1 = \delta y = 0$, and if stability E is defined as the resistance by the atmosphere, per unit distance, to unstable accelerations,

$$E_v = B(B - \partial u_g/\partial z) + (g/\theta)(\partial\theta/\partial z) \,. \quad (9)$$

This agrees with the previous expression for stability, Eq 3.17(3), except for the term with B. Since $2\omega\cos\theta$ has maximum value 1.46×10^{-4} sec^{-1}, while $\partial u_g/\partial z$ is usually in the range of magnitude 10^{-3} to 10^{-2} sec^{-1}, and the last term on the right is of the order 10^{-5} to 10^{-4} sec^{-2}, Eq (9) reduces to

$$E_v \simeq (g/\theta)(\partial\theta/\partial z) \,. \quad (10)$$

In retrospect, it is evident that, although Eq (10) is the standard definition for stability, it does not express completely the stability along the vertical.

Inertia stability E_h is defined from Eq (5).

$$E_h = -(1/\delta y)(dv/dt)_A \simeq (2\omega\sin\phi) \times (2\omega\sin\phi - \partial u_g/\partial y) \,. \quad (11)$$

As $2\omega\sin\phi$ is positive (northern hemisphere), the atmosphere has inertia stability or instability according as $\partial u_g/\partial y \lessgtr 2\omega\sin\phi$. The sign of inertia stability is dependent only on relative values of the Coriolis parameter and the horizontal shear of geostrophic wind. *There can be inertia instability only when the shear is negative (anticyclonic) and of magnitude exceeding the Coriolis parameter.* In middle latitudes this requires anticyclonic shear about 10^{-4} sec^{-1} or greater. Since that shear seldom is so large, the atmosphere is characterized generally by inertia stability. However, there is one region of the atmosphere in particular where inertia instability frequently exists, namely, immediately to the right of jet streams where anticyclonic shear can be large.

Eq (11) is a valid expression for inertia stability only when the quantity (from Eq [5]) $-f(B - \partial u_g/\partial z)(\delta z/\delta y) - Cw_1/\delta y$ is negligible. This would be the case with no vertical displacements ($\delta z = w_1 = 0$). In regions of strong vertical shear of geostrophic wind the first term above can be large even with small vertical displacements. In such conditions it would have to be considered along with the term retained in Eq (11).

In regions where inertia instability exists, conditions are favorable for horizontal mixing. An air parcel deflected from the geostrophic flow would develop transverse acceleration, carrying it farther away from its original position in the current, and theoretically it could not come to equilibrium with the pressure field until it arrived in a region of stability. All this suggests that regions of strong anticyclonic shear are favorable for horizontal mixing and that inertia instability might be part of the explanation for the weak temperature field to the right of the strong wind current in Figure 7.08*b*.

For the reader interested in reviewing the subject of stability as related to lateral displacements in more detail, we mention a few of the previous works: Solberg,[32] Van Meigham,[33] Palmén,[34] Godson,[35] and Bjerknes.[36]

32. H. Solberg, "Le Mouvement d'inertie de l'atmosphère stable et son rôle dans la théorie des cyclones," *Procès-verbaux de l'assoc. de météor., U.G.G.I., Edimbourg*, 1936, pp. 66–82.

33. J. Van Meigham, "Perturbation d'un courant atmosphérique permanent zonal," *Inst. R. météor. Belg.*, Mem., XVIII (1944), 1–34; "Hydrodynamic Instability," in American Meteorological Society, *Compendium of Meteorology*, pp. 434–53.

34. E. Palmén, "On the Distribution of Temperature and Wind in the Upper Westerlies," *Journal of Meteorology*, Vol. V, No. 1.

35. W. L. Godson, "Generalized Criteria for Dynamic Instability," *Journal of Meteorology*, VII (1950), 268–78; "Synoptic Significance of Dynamic Instability," *ibid.*, pp. 333–42.

36. J. Bjerknes, "Extratropical Cyclones," in American Meteorological Society, *Compendium of Meteorology*, pp. 577–98.

READING REFERENCES

Byers, H. R. *General Meteorology*, Chap. 16. New York: McGraw-Hill Book Co., 1944.

Petterssen, Sverre. *Weather Analysis and Forecasting*, pp. 205–21, 378–440. New York: McGraw-Hill Book Co., 1940.

四、4　補充資料-2
(江火明老師之天氣學講義)

6、C 第六章 高空等壓面天氣圖的分析

§ 6-1 前言

對大氣熱力性質的瞭解，必須分析氣壓場、氣溫場、濕度場、密度場與位溫場。

若大氣適合流體靜力平衡，則氣壓與高度為1-1單調遞減函數，故可以選擇氣壓為垂直座標。在等壓面上，高度較大的地方就相當於等高面上的高壓位置；高度較低的地方就相當於等高面上的低壓位置。

$p=\rho RT$

在等壓面上，由於理想氣體方程式知，①密度只是氣溫的函數，等密度線必平行等溫線，故不需再做密度場的分析；②又由位溫的定義，在等壓面上等位溫線必平行等溫線，故不需再做位溫場的分析。因此，若高空天氣圖選擇等壓面圖，則只要分析高度場、氣溫場與濕度場即可。在分析作業上方便很多。

$\left(\frac{P_{00}}{P}\right)^{R/C_p}$

對於中高緯度地區，大尺度大氣運動適合準地轉近似，故高度場即為準地轉運動的流場。

$\theta = T\left(\frac{P_{00}}{P}\right)^{R/C_p}$

$\nabla^2\psi = \zeta = \frac{1}{f}\nabla^2\Phi \Rightarrow \psi' = \frac{\Phi'}{f}$ (geostrophy)

§ 6-2 地轉風與高度場的分析

若大氣運動適合地轉風近似，在等壓面上地轉風的大小可以下式表之：

$$V_g = \frac{g}{f}\left(\frac{\partial z}{\partial n}\right) = \frac{g}{f}\frac{\delta z}{\delta n}, \tag{6-1}$$

若已知地轉風的大小，且相隔(鄰)兩條等高線的距離為 δn，兩相鄰等高線之數值差為δz（一般取60 gpm），則

$$\delta n = \frac{g}{f}\frac{\delta z}{V_g}, \tag{6-2}$$

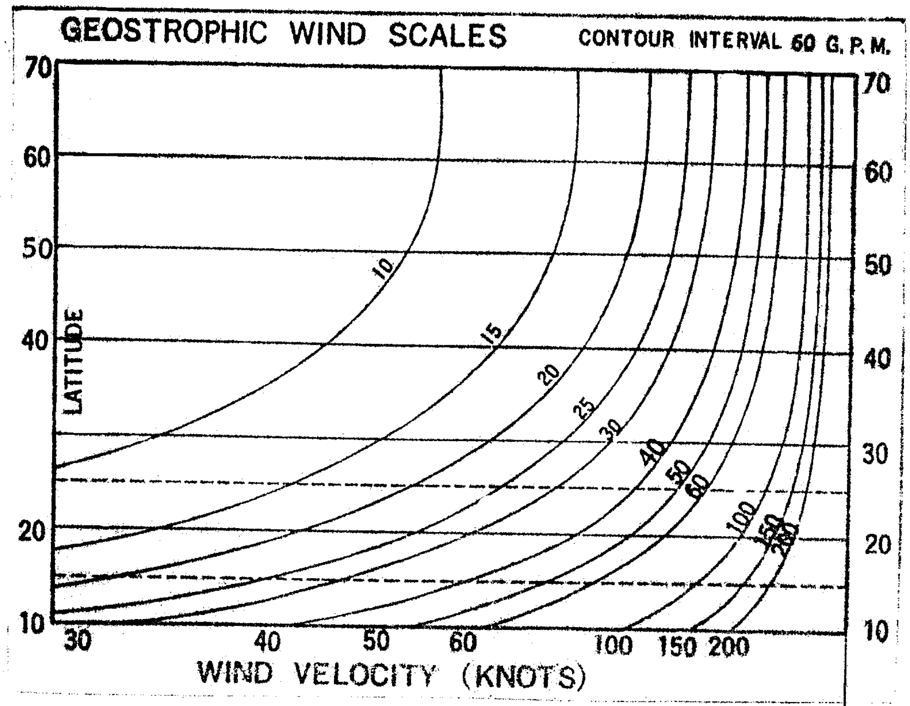

δn

圖6 -1

∴同樣之δn，越高緯風速越小

利用上式可繪製圖6 -1，由圖中可查出不同緯度之相隔兩條等高線的距離與其間地轉風大小的關係。在高空天氣圖分析時，要多利用地轉風大小來修正~~兩~~修等高線間的距離。

當然，實際風與地轉風間有差異的，其向量差稱為地轉偏差風（Ageostrophic Wind, $\vec{V}_{ag}$ ），即

or（非地轉風，擬地轉風）

$$\vec{V}_{ag} = \vec{V} - \vec{V}_g \quad , \qquad (6\text{-}3)$$

決定$\vec{V}_{ag}$ 的因素有（1）地形；（2）摩差力作用；（3）發展迅速的天氣系統。

（对流地転偏差風）

在北半球中高緯度地區，大尺度大氣運動近似地轉平衡，因此，在高壓（ℍ）地區氣流呈反氣旋運動，在低壓（𝕃）地區氣流呈氣旋運動。

在高空圖上，中高緯度地區處於顯著西風帶，大尺度大氣運動表示出明顯的羅士培波（Rossby Waves）的型式，因此，在分析高度場時，要特別留意脊（Ridge）與槽（Trough）的位置。

(3) § 6-3 熱力風與厚度場（溫度場）的分析

溫度是無向量，它的分析可依第四章的要點分析之。由流體靜力平衡關係知，兩等壓面之厚度正比於此層大氣之平均溫度。即 $\frac{\partial z}{\partial p} = -\frac{RT}{p}$

兩等壓面上地轉風之向量差，定義為這層大氣的熱力風（Thermal Wind, $\vec{V}_T$）向量，即

$$\vec{V}_T = \vec{V}_{g,U} - \vec{V}_{g,L} \quad , \qquad \vec{V}_g = -\frac{g}{f}\hat{k}\times\nabla_p Z \,, \qquad \therefore \frac{\partial \vec{V}_g}{\partial p} = -\frac{g}{f}\hat{k}\times\nabla_p\left(\frac{\partial z}{\partial p}\right) = \frac{R}{fp}\hat{k}\times\nabla_p T \qquad (6\text{-}3)$$

其中，$\vec{V}_{g,U}$ 與 $\vec{V}_{g,L}$ 分別為上層與下層的地轉風分量。~~地轉~~熱力風的大小可以下式表之：

$$V_T = \frac{g}{f}\left(\frac{\partial \Delta z}{\partial n}\right) = \frac{g}{f}\frac{\delta \Delta z}{\delta n} \,, \qquad (6\text{-}4)$$

因此，$\vec{V}_T$ 與 Δz 的關係就相當於 $\vec{V}_g$ 與 z 的關係。同樣的可以利用圖6-1，查出不同緯度之相隔兩條等厚度線的距離，來判斷熱力風的大小。

在正壓的區域，風速與氣流的形勢都不隨高度改變，即

$$\frac{\partial \vec{V}_T}{\partial z} = 0 \,, \qquad (6\text{-}5)$$

由 $\frac{\partial \vec{V}_g}{\partial p} = \frac{R}{fp}\hat{k}\times\nabla_p T \Rightarrow \begin{cases} \frac{\partial u_g}{\partial p} = \frac{R}{fp}\left(\frac{\partial T}{\partial y}\right)_p \\ \frac{\partial v_g}{\partial p} = \frac{-R}{fp}\left(\frac{\partial T}{\partial x}\right)_p \end{cases} \Rightarrow$ ∴等壓面上南北溫度梯度之大小，與垂直方向之西風梯度成正比。一般在中緯度有最大之 $\frac{\partial T}{\partial y}$，故其上層之 u_g 亦最強（噴流）。另外在夏季之南亞地區上空，∵青藏高原之加熱作用，使得此區之 $\frac{\partial T}{\partial y}$ 反向且很強，故此區之上空有東風噴流。

若氣流形勢與氣溫形勢同~~向~~相位，即等壓面上的高度槽就是溫度槽，則地轉風風向不隨高度改變；風速隨高度遞增，這也表示熱力風與下層風同向。由於

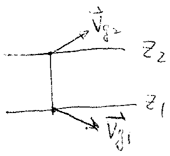

$$\vec{V}_T = \frac{-R}{f}\int_{p_U}^{p_L}(\hat{k}\times\nabla T)\,d\ln p \quad , \tag{6-6}$$

∵ 噴流處 ∇T 大
鋒面処，∵∇T 大 ⇒ ∴有上層噴流

表故熱力風風向總是平行於溫度線，在北半球，背對著風向，在其左側為冷側；右側為暖側。若空氣由冷側吹向暖側，即冷平流，則上層地轉風在下層地轉風的左側，換句話說，風向隨高度增高呈逆時針方向改變（冷平流）；若空氣由暖側吹向冷側，即暖平流，則上層地轉風在下層地轉風的右側，換句話說，風向隨高度增高呈順時針方向改變。（暖平流）熱力風之討論对单站之探空資料之分析有很大之幫助。∵它有助於研判一~~冷或暖~~天气系统是否在移近或移出。→（接上页背面）

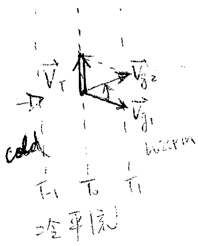

$\boxed{59b}$ 续 p.60 中間.

* 厚度場之変化和平均溫度之関係：

由流体静力平衡方程式：

$$\int dz = \int -\frac{RT}{gp}\,dp$$

$$\Rightarrow z_2 - z_1 = +\frac{R}{g}\int_{p_2}^{p_1} T\,d\ln p = \frac{R}{g}\,\bar{T}\,\ln\frac{p_1}{p_2}$$

$$故\ \left(\frac{\partial z}{\partial t}\right)_2 - \left(\frac{\partial z}{\partial t}\right)_1 = \frac{R}{g}\left(\ln\frac{p_1}{p_2}\right)\frac{\partial \bar{T}}{\partial t}.$$

即兩等压面之高度变化趨勢的差（厚度趨勢），只和其間之平均溫度的变化趨勢成正比。

若兩等压面間之溫度不变，則此二等压面之高度变化趨勢相等。$\left(\frac{\partial z_2}{\partial t} = \frac{\partial z_1}{\partial t}\right)$

若 〃 〃 〃 〃 〃 溫度增高，則会使等压面向上抬升，且上層比下層抬升更高。

若 〃 〃 〃 〃 〃 溫度降低，則 $\left(\frac{\partial z}{\partial t}\right)_2 < \left(\frac{\partial z}{\partial t}\right)_1$，且 Δz_2 比 Δz_1 要下降得多、即兩等压面間之厚度減小。
$\left(\frac{\partial \bar{T}}{\partial t} < 0\right.$，冷平流）　（冷平流）

溫度增高，$\frac{\partial \bar{T}}{\partial t} > 0$，則 $\frac{\partial z_2}{\partial t} > \frac{\partial z_1}{\partial t}$，且 Δz_2 比 Δz_1 上升得多，厚度变大。
暖平流　（暖平流）

9、C(4)
§ 6 - 4 等壓面上脊（或ℍ）、槽（或𝕃）隨高度的傾斜

如圖 6 - 2，若b 與a 分別為p_1面與p_2面的兩個等壓面上的兩點，在這兩點之等壓面斜率（$(\frac{\partial z}{\partial s})_p$）相等，我們欲探討這天氣系統隨高度遞增而傾斜的情形。圖6 - 2 為$(\frac{\partial z}{\partial s})_p$ = Const. 的位置隨高度的變化圖。

由流體靜力平衡，

$$\frac{\partial z}{\partial p} = -\frac{\alpha}{g}, \tag{6-7}$$

故得

$$\delta z = -\frac{\alpha}{g}\delta p, \tag{6-8}$$

即

$$z_b - z_a = -\frac{\alpha}{g}\delta p, \tag{6-9}$$

其中 $\delta p = p_1 - p_2$ (6-10)

(§8.2)
① 大动 之 2-layer model ; tendency eq (§6.3)
② tanψ (over)
③ ~~[illegible]~~ ~~[illegible]~~
④ §6-4 (here)

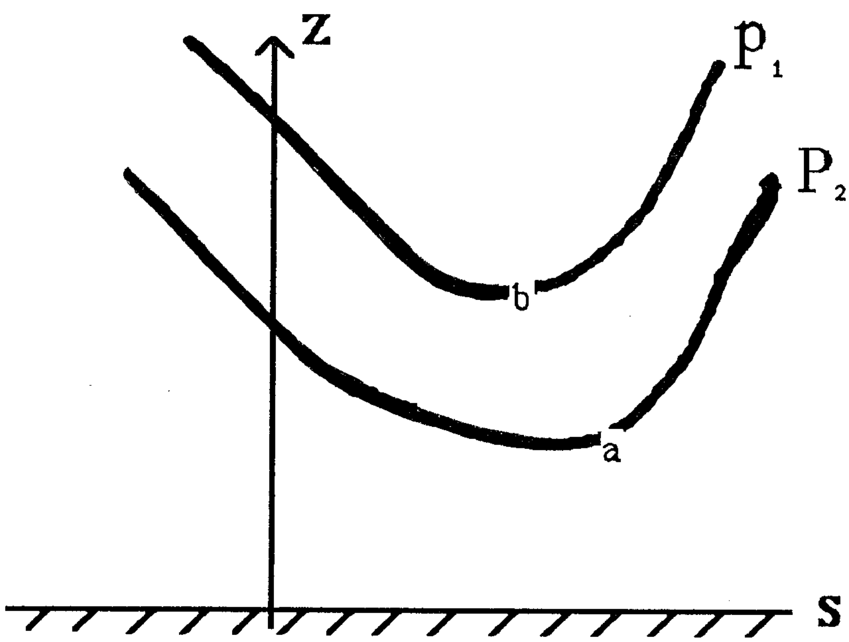

圖 6-2

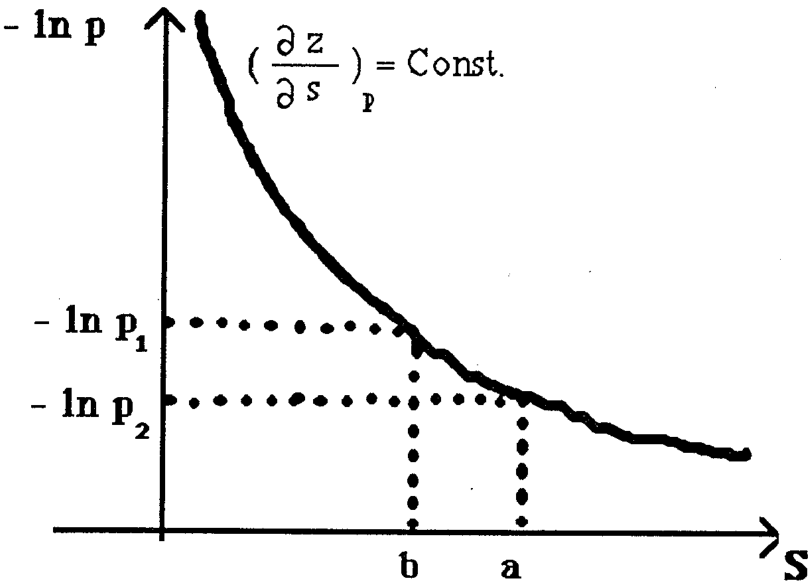

圖 6–3

又因$(\frac{\partial z}{\partial s})$是s與p的函數，故

$$\delta\left(\frac{\partial z}{\partial s}\right) = \left(\frac{\partial}{\partial s}\right)\left(\frac{\partial z}{\partial s}\right)\delta s + \left(\frac{\partial}{\partial p}\right)\left(\frac{\partial z}{\partial s}\right)\delta p$$

$$= (\frac{\partial^2 z}{\partial s^2})\,\delta s - (\frac{\partial \alpha}{\partial s})\frac{\delta p}{g} \quad , \tag{6-11}$$

對等壓面斜率相同的位置，

$$(\frac{\partial z}{\partial s})_b - (\frac{\partial z}{\partial s})_a = (\frac{\partial^2 z}{\partial s^2})\,\delta s - (\frac{\partial \alpha}{\partial s})\frac{\delta p}{g}$$

$$= 0 \quad , \tag{6-12}$$

故得

$$\frac{\delta p}{\delta s} = g\,\frac{(\frac{\partial^2 z}{\partial s^2})_p}{(\frac{\partial \alpha}{\partial s})_p} \tag{6-13}$$

即 $$\frac{\delta z}{\delta s} = -\,\frac{(\frac{\partial^2 z}{\partial s^2})_p}{(\frac{1}{\alpha})(\frac{\partial \alpha}{\partial s})_p} \quad , \because \delta p = -\frac{g}{\alpha}\,\delta z \quad (6\text{-}8)$$

$$= -\,\frac{(\frac{\partial^2 z}{\partial s^2})_p}{(\frac{1}{T})(\frac{\partial T}{\partial s})_p} \tag{6-14}$$

等壓面上，

$$(\frac{\partial^2 z}{\partial s^2})_p > 0\text{，在槽（或}\mathbb{L}\text{）處；}$$

$$(\frac{\partial^2 z}{\partial s^2})_p < 0\text{，在脊（或}\mathbb{H}\text{）處；} \tag{6-15}$$

故槽（或$\mathbb{L}$）隨高度遞增而傾斜的斜率為

$$\frac{\delta z}{\delta s} = -\,\frac{\left|(\frac{\partial^2 z}{\partial s^2})_p\right|^{(+)}}{(\frac{1}{T})(\frac{\partial T}{\partial s})_p} \tag{6-16}$$

脊（或$\mathbb{H}$）隨高度遞增而傾斜的斜率為

$$\frac{\delta z}{\delta s} = \frac{\left|(\frac{\partial^2 z}{\partial s^2})_p\right|^{(-)}}{(\frac{1}{T})(\frac{\partial T}{\partial s})_p} \tag{6-17}$$

(6-16) 與 (6-17)兩式的分母，表示斜壓性的大小，在正壓的情況，$(\frac{\partial T}{\partial s})_p=0$，則脊（或ℍ）、槽（或𝕃）隨高度遞增並無傾斜的現象。在斜壓性很强的地方，則 $\frac{\delta z}{\delta s}$ 很小，即脊（或ℍ）、槽（或𝕃）隨高度遞增傾斜很厲害。

若 $(\frac{\partial T}{\partial s})_p > 0$，則

(1) 在脊（或ℍ）處，$\frac{\delta z}{\delta s} > 0$，即脊隨高度遞增向+δs（暖側）傾斜；

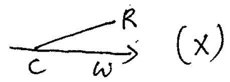

(2) 在槽（或𝕃）處，$\frac{\delta z}{\delta s} < 0$，即槽隨高度遞增向-δs（冷側）傾斜。

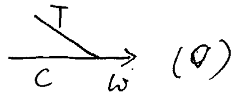

若 $(\frac{\partial T}{\partial s})_p < 0$，則

(南北半球均向西傾斜) $\therefore \frac{\partial z}{\partial s} < 0$

(1) 在脊（或ℍ）處，$\frac{\delta z}{\delta s} < 0$，即脊隨高度遞增向-δs（暖側）傾斜；

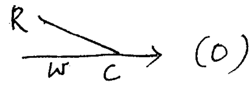

(2) 在槽（或𝕃）處，$\frac{\delta z}{\delta s} > 0$，即槽隨高度遞增向+δs（冷側）傾斜。

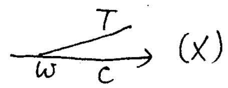

換言之，高壓中心（或脊）總是隨高度遞增傾向暖側；低壓中心（或槽）總是隨高度遞增傾向冷側。 $(\frac{\partial^2 z}{\partial x^2})$

由 (6-16) 與 (6-17)兩式知，等壓面曲率很大的天氣系統（脊、槽、ℍ、𝕃），亦即很顯著的上凸或下凹的天氣系統，它隨高度遞增而傾斜較小（$\frac{\delta z}{\delta s}$ 大）；若是較平淺的天氣系統，它隨高度遞增而傾斜很厲害（$\frac{\delta z}{\delta s}$ 小）。

若𝕃₁, 𝕃₂兩圓形低壓中心，等壓面向上彎曲的曲率相同，在𝕃₁附近溫度梯度大；而在𝕃₂附近溫度梯度小，則𝕃₁隨高度遞增向冷側傾斜較厲害。

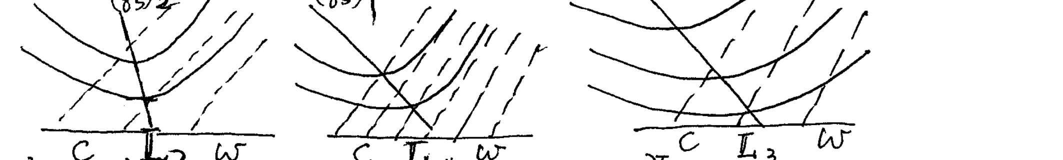

$(\frac{\partial^2 z}{\partial x^2})_1 = (\frac{\partial^2 z}{\partial x^2})_2$
$(\frac{\partial T}{\partial s})_2 < (\frac{\partial T}{\partial s})_1$ $\therefore (\frac{\delta z}{\delta s})_2 > (\frac{\delta z}{\delta s})_1$

$(\frac{\partial T}{\partial s})_1 = (\frac{\partial T}{\partial s})_3$
$(\frac{\partial^2 z}{\partial x^2})_1 > (\frac{\partial^2 z}{\partial x^2})_3 \Rightarrow (\frac{\delta z}{\delta s})_1 > (\frac{\delta z}{\delta s})_3$

若$\mathbb{L}_1$, $\mathbb{L}_3$兩圓形低壓中心附近溫度梯度相同，在$\mathbb{L}_1$等壓面向上彎曲的曲率大（等壓線較密集）；而在$\mathbb{L}_3$等壓面向上彎曲的曲率小（等壓線較疏寬），則$\mathbb{L}_3$隨高度遞增向冷側傾斜較厲害。

換句話說，一圓形氣旋（反氣旋）中心隨高度遞增偏向冷（暖）側傾斜，若高度一定，則偏移的大小 δs 與溫度梯度成正比；與等壓面向上（下）彎曲的曲率成反比。

C、(5)　(由地形、摩擦力、氣層中之各種等因素造成地轉偏差風)

§ ~~6—6~~ 地轉偏差運動　(Ref. p.240 (§7.23) of Saucier, 1955)

由地轉偏差風之定义，$\vec{V}_{ag}=\vec{V}-\vec{V}_g$，及地轉風 $f\hat{k}\times\vec{V}_g=-\nabla_p\Phi$

∴運動方程式：$\frac{d\vec{V}}{dt}=-f\hat{k}\times\vec{V}-\nabla_p\Phi+\vec{F}_r=-f\hat{k}\times(\vec{V}-\vec{V}_g)+\vec{F}_r$

(即空氣之加速度是由科氏力、壓力梯度力及摩擦力之不平衡所造成。)
若三力平衡，則加速度為0.

$$\Rightarrow \frac{d\vec{V}}{dt}=-f\hat{k}\times\vec{V}_{ag}+\vec{F} \qquad (6\text{-}20)$$

$\vec{F}=0$

若大氣無摩擦力的作用，則單位質量大氣的地轉偏差風的柯氏力，即為大氣運動的加速度。

$(\vec{V} > \vec{V}_g)$

若眞實風與地轉風同向，但風速卻大於地轉風風速，即超地轉風（Supergeostrophic Wind），則地轉偏差分量與眞實風同向，由(6-20)式知地轉偏差風的柯氏力向眞實風的右側，故超地轉風（Supergeostrophic Wind）使大氣運動向右加速。

$\vec{V} < \vec{V}_g$

若眞實風與地轉風同向，但風速卻小於地轉風風速，即次地轉風（Subgeostrophic Wind），則地轉偏差分量與眞實風反向，由(6-20)式知地轉偏差風的柯氏力向眞實風的左側，故次地轉風（Subgeostrophic Wind）使大氣運動向左加速。

由定義知

$$\vec{V} = \vec{V}_g + \vec{V}_{ag} \tag{6-21}$$

0，无摩擦作用时、

$$\frac{d\vec{V}}{dt} = \frac{d\vec{V}_g}{dt} + \frac{d\vec{V}_{ag}}{dt} = -f\hat{k} \times \vec{V}_{ag} + \cancel{\vec{F}}$$

$$= \frac{\partial \vec{V}_g}{\partial t} + \vec{V} \cdot \nabla \vec{V}_g + \omega \frac{\partial \vec{V}_g}{\partial p} + \frac{d\vec{V}_{ag}}{dt} \tag{6-22}$$

故

$$-f\hat{k} \times \vec{V}_{ag} = \frac{\partial \vec{V}_g}{\partial t} + \vec{V} \cdot \nabla \vec{V}_g + \omega \frac{\partial \vec{V}_g}{\partial p} + \frac{d\vec{V}_{ag}}{dt} - \vec{F}_r \tag{6-23}$$

即

$$\hat{i}: \quad v_{ag}\cancel{u}_{ag} = \frac{1}{f}\frac{\partial u_g}{\partial t} + \frac{u}{f}\frac{\partial u_g}{\partial x} + \frac{v}{f}\frac{\partial u_g}{\partial y} + \frac{\omega}{f}\frac{\partial u_g}{\partial p} - \frac{1}{f}F_x + \frac{1}{f}\frac{du_{ag}}{dt} \tag{6-24a}$$

$$\hat{j}: \quad u_{ag}\cancel{v}_{ag} = \underbrace{-\frac{1}{f}\frac{\partial v_g}{\partial t}}_{(1)} \underbrace{- \frac{u}{f}\frac{\partial v_g}{\partial x} - \frac{v}{f}\frac{\partial v_g}{\partial y}}_{(2)} \underbrace{- \frac{\omega}{f}\frac{\partial v_g}{\partial p}}_{(3)} \underbrace{+ \frac{1}{f}F_y}_{(4)} \underbrace{- \frac{1}{f}\frac{dv_{ag}}{dt}}_{(5)} \tag{6-24b}$$

此即表示地轉偏差風可分為五個分量：（1）等變壓風分量（Isollobaric Wind）；（2）平流地轉偏差風分量（Advective Ageostrophic Wind）；（3）對流地轉偏差風分量（Convective Ageostrophic Wind）；（4）摩擦地轉偏差風分量（Antitriptic Wind）；（5）地轉偏差變量分量。亦即

$$\vec{V}_{ag} = \vec{V}_{ag(i)} + \vec{V}_{ag(a)} + \vec{V}_{ag(c)} + \vec{V}_{ag(F)} + \vec{X} \tag{6-25}$$

See Holton (§6.4)

(一) 摩擦地轉偏差風分量（Antitriptic Wind）

摩擦力為減速力，它使空氣運動的速度減小，科氏力也隨之減小，但壓力梯度力不受影響（壓力場沒有變化），如圖，科氏力、梯度力（壓力）與摩擦力平衡，因

$$-f\hat{k}\times\vec{V}_{ag(F)} = -\vec{F} \quad (\text{在無加速度時 } \frac{d\vec{V}}{dt}=0) \qquad (6\text{-}26)$$

故摩擦力與摩擦地轉偏差風分量之科氏力，大小相等方向相反。因此，真實風總是比地轉風小，在北半球它偏向地轉風的左側。(即指向低壓)

且 總

陸地上約為 40%
海上 約 60%

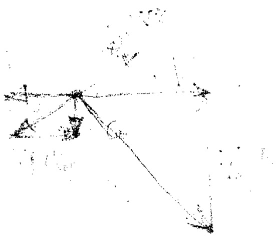

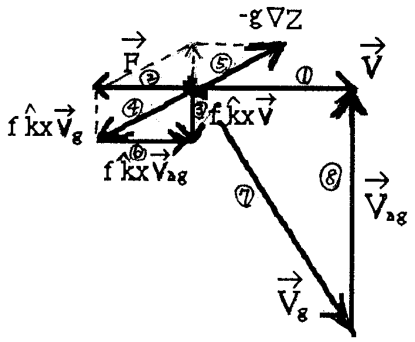

圖 6-5

(二) 等變壓風分量（Isollobaric Wind）

$\nabla(\frac{\partial Z}{\partial t})$ app. $\quad \vec{V}_{ag(i)} = \frac{1}{f}\hat{k}\times\frac{\partial\vec{V}_g}{\partial t}$

當等變壓線($\nabla(\frac{\partial Z}{\partial t})$)的梯度很大時，等變壓風分量可能是地轉偏差風的主要部分。因 (地轉風隨時間之變化 → 如系統之發展等)

$$-f\hat{k}\times\vec{V}_{ag(i)} = \frac{\partial\vec{V}_g}{\partial t} \Rightarrow \vec{V}_{ag(i)} = \frac{1}{f}\hat{k}\times\frac{\partial\vec{V}_g}{\partial t} \qquad (6\text{-}27)$$

由地轉平衡方程式

$$\left(-f\hat{k}\times\vec{V}_g = g\nabla Z\right) \quad \because \vec{V}_g = +\frac{g}{f}\hat{k}\times\nabla Z \quad \begin{cases} u_g = -\frac{1}{f}\frac{\partial\Phi}{\partial y} \\ v_g = \frac{1}{f}\frac{\partial\Phi}{\partial x}\end{cases} \qquad (6\text{-}28)$$

故

$$\Rightarrow \vec{V}_{ag(i)} = \frac{1}{f}\hat{k}\times\frac{\partial\vec{V}_g}{\partial t} \qquad [\because \hat{k}\times(\hat{k}\times\vec{V}) = -\vec{V}]$$

$$= -\frac{g}{f^2}\frac{\partial\nabla Z}{\partial t}$$

$$-f\hat{k} \times \frac{\partial \vec{V}_g}{\partial t} = g \nabla \frac{\partial Z}{\partial t} \qquad (6\text{-}29)$$

因此

$$g \nabla \frac{\partial Z}{\partial t} = -f^2 \vec{V}_{ag(i)} \qquad (6\text{-}30)$$

$\frac{\partial}{\partial t}(\nabla Z)$ $-\nabla(\frac{\partial Z}{\partial t})$

此即表示 $\vec{V}_{ag(i)}$ 與等變高線的梯度成正比，而方向指向等高線下降的一側。(即指向低压)

（三）平流地轉偏差風分量（Advective Ageostrophic Wind）

氣塊平移時，因等高線的曲率不同，即不平行，故移行的軌跡與等高線間有差異，如圖6-6所示，

即当一気塊平移时，雖然在開始可達地轉(or gradient)平衡，但平移後，馬上進入另一种压力梯度力，使其失去原有之平衡，故気塊必须調節自己，使其再度達到新的平衡，這种調節之过程，即会產生加速度，因此產生了非地轉之分量来。

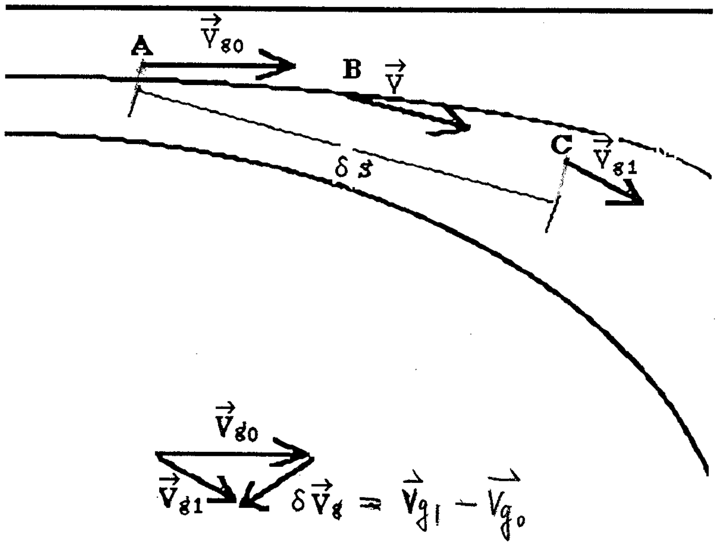

圖 6-6

因

$$-f\hat{k} \times \vec{V}_{ag(a)} = \vec{V} \cdot \nabla \vec{V}_g = |\vec{V}_B| \frac{\delta \vec{V}_g}{\delta s} \qquad (6\text{-}31)$$

or $\vec{V}_{ag(a)} = \frac{|\vec{V}_B|}{f} \hat{k} \times \frac{\delta \vec{V}_g}{\delta s}$

故 $\vec{V}_{ag(a)}$ 與 $\delta\vec{V}_g$ 垂直，且在其左側。$\delta\vec{V}_g$ 有兩個分量，一垂直於 $\vec{V}_B$，它使風轉向，以趨向於平~~行~~高的等高線；另一在 $\vec{V}_B$ 的反(同)向，它使風速減小(增强)，在分流区(合流区)。~~以趨向分流等高線的梯度一致~~。因此，在分流處平流地轉偏差風分量偏向高壓；在合流處平流地轉偏差風分量偏向低壓。（如圖6-7）

$\because \vec{V}_{ag} = \frac{|\vec{V}_B|}{f}\hat{k}\times\frac{\delta\vec{V}_g}{\delta s}$

① 由 $\vec{V}_{g0}$ 及 $\vec{V}_{g1}$ 得 $\delta\vec{V}_g$

② 由 $\hat{k}\times\delta\vec{V}_g$ 得 $\vec{V}_{ag}$ #

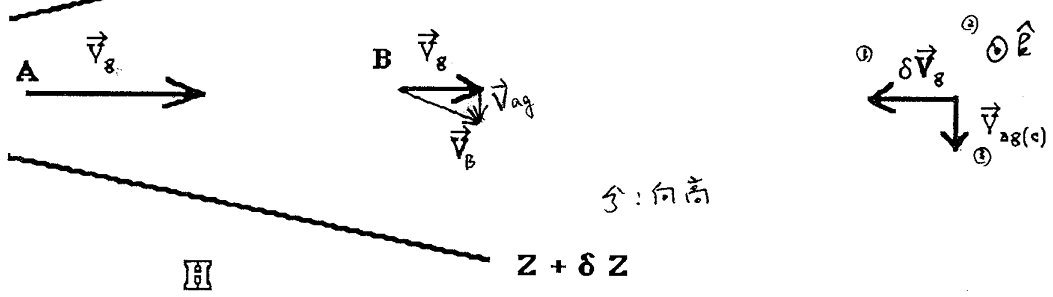

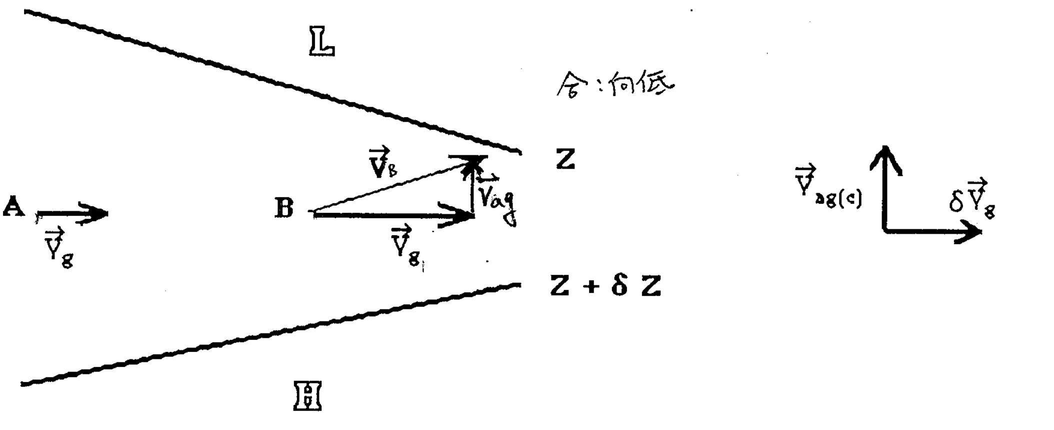

圖 6-7

⇒ 風速变小時(分流)，$\vec{V}_{ag}$指向右，∴$\vec{V}$会向右偏，偏離低压。

風速变大时(合流)，$\vec{V}_{ag}$指向左，∴$\vec{V}$会向左偏，偏向低压。

⇒ 均趨向於平行高的等高线。

（四）對流地轉偏差風分量（Convective Ageostrophic Wind）

因為

$$-f\hat{k} \times \vec{V}_{ag(c)} = \omega\frac{\partial \vec{V}_g}{\partial p} = \omega\frac{\delta \vec{V}_g}{\delta p} \Rightarrow \vec{V}_{ag(c)} = \frac{\omega}{f}\hat{k}\times\frac{\delta \vec{V}_g}{\delta p} \quad (6\text{-}32)$$

$\ominus\uparrow$ $\oplus\downarrow$ → 熱力風

故在上升運動（$\omega<0$）處，$\omega\frac{\partial \vec{V}_g}{\partial p}$ 與 $\delta\vec{V}_g$ 同向，$\vec{V}_{ag(c)}$ 在 $\delta\vec{V}_g$ 的左側（冷側），即若氣流上升，則對流地轉偏差風與等溫~~濾~~线相交，且指向冷側；在下降運動（$\omega>0$）處，$\omega\frac{\partial \vec{V}_g}{\partial p}$ 與 $\delta\vec{V}_g$ 反向，$\vec{V}_{ag(c)}$ 在 $\delta\vec{V}_g$ 的右側（暖側），即若氣流下降，則對流地轉偏差風與等溫~~濾~~线相交，且指向暖側（如圖 6-8）。強烈的溫度水平梯度與垂直運動，將伴隨強盛的 $\vec{V}_{ag(c)}$。

$\frac{\delta \vec{V}_g}{\delta p}$

∴在垂直速度大之地區，如鋒面或山坡附近，及水平溫度梯度大之地區，如鋒面或海陸交界地區，均有強烈之此項效應。

上升運動 $\vec{V}_{ag}$ 指向冷區
下降運動 $\vec{V}_{ag}$ 指向暖區

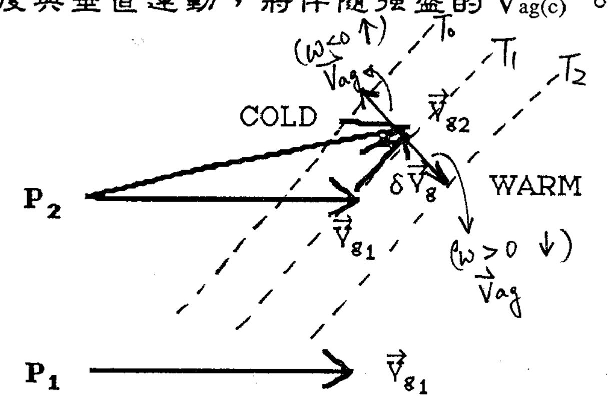

圖 6-8

（五）加速度

$$-f\hat{k}\times\vec{V}_{ag(x)} = \frac{d\vec{V}_{ag}}{dt}$$

$$\frac{d\vec{V}_{ag}}{dt} = -f\hat{k}\times\vec{V}_{ag} \Rightarrow$$ ∴科氏加速力使其向右偏。#